

DO-TH 95/13

RAL-TR-95-042

August 1995

updated version (December 1995)

Next-to-Leading Order Radiative Parton Model Analysis of Polarized Deep Inelastic Lepton Nucleon Scattering

M. Glück, E. Reya, M. Stratmann

Universität Dortmund, Institut für Physik,
D-44221 Dortmund, Germany

W. Vogelsang

Rutherford Appleton Laboratory
Chilton, Didcot, Oxon OX11 0QX, England

Abstract

A next-to-leading order QCD analysis of spin asymmetries and structure functions in polarized deep inelastic lepton nucleon scattering is presented within the framework of the radiative parton model. A consistent NLO formulation of the Q^2 -evolution of polarized parton distributions yields two sets of plausible NLO spin dependent parton distributions in the conventional $\overline{\text{MS}}$ factorization scheme. They respect the fundamental positivity constraints down to the low resolution scale $Q^2 = \mu_{NLO}^2 = 0.34 \text{ GeV}^2$. The Q^2 -dependence of the spin asymmetries $A_1^{p,n,d}(x, Q^2)$ is similar to the leading-order (LO) one in the range $1 \leq Q^2 \leq 20 \text{ GeV}^2$ and is shown to be non-negligible for x -values relevant for the analysis of the present data and possibly forthcoming data at HERA.

1 Introduction

Recently, a leading order (LO) QCD analysis of polarized deep inelastic lepton nucleon scattering has been performed [1] within the framework of the radiative parton model. The first moments $\Delta f(Q^2)$ of polarized parton distributions $\delta f(x, Q^2)$,

$$\Delta f(Q^2) \equiv \int_0^1 dx \delta f(x, Q^2) \quad , \quad (1.1)$$

where $f = u, \bar{u}, d, \bar{d}, s, \bar{s}, g$, were subject to two very different sets of theoretical constraints related to two different views concerning the flavor $SU(3)$ [$SU(3)_f$] symmetry properties of hyperon β -decays. One set ('standard' scenario) assumed an unbroken $SU(3)_f$ symmetry between the relevant matrix elements while the other set ('valence' scenario) assumed an extremely broken $SU(3)_f$ symmetry reflected in relating [2] the hyperon β -decay matrix elements to the first moments of the corresponding *valence* distributions. Both scenarios gave satisfactory descriptions [1] of the measured spin-asymmetries [3-9] $A_1^{p,n}(x, Q^2) \simeq g_1^{p,n}(x, Q^2)/F_1^{p,n}(x, Q^2)$, although the polarized gluon density $\delta g(x, Q^2)$, which enters in LO only via the Q^2 -evolution equations, was only weakly constrained by present data. The total helicity carried by quarks

$$\Delta\Sigma(Q^2) \equiv \sum_{q=u,d,s} (\Delta q(Q^2) + \Delta\bar{q}(Q^2)) \quad , \quad (1.2)$$

which is Q^2 -independent in LO, turned out to be $\Delta\Sigma \simeq 0.3$ in both scenarios with an average total gluonic helicity $\Delta g(Q^2 = 4 \text{ GeV}^2) \simeq 1.5$. A specific feature of our radiative LO analysis is that the polarized leading twist parton densities $\delta f(x, Q^2)$ are valid down to $Q^2 = \mu_{LO}^2 \simeq 0.23 \text{ GeV}^2$ and that the fundamental positivity constraints

$$|\delta f(x, Q^2)| \leq f(x, Q^2) \quad (1.3)$$

are respected down to this low resolution scale $Q^2 = \mu_{LO}^2$ as well. The 'standard' scenario requires a finite total strange sea helicity of $\Delta s = \Delta\bar{s} \simeq -0.05$ in order to account for a reduction of Γ_1^p with respect to the Gourdin and Ellis and Jaffe estimate [10]

$$\Gamma_{1,EJ}^p = \frac{1}{12}(F + D) + \frac{5}{36}(3F - D) \simeq 0.185 \quad (1.4)$$

where

$$\Gamma_1^p(Q^2) \equiv \int_0^1 dx g_1^p(x, Q^2) \quad . \quad (1.5)$$

Within the 'valence' scenario, on the contrary, a negative light sea helicity $\Delta\bar{u} = \Delta\bar{d} \equiv \Delta\bar{q} \simeq -0.07$ suffices ($\Delta s = \Delta\bar{s} = 0$) for reducing $\Gamma_{1,EJ}^p$. Furthermore, in both scenarios we [1] predict $\Gamma_1^p \simeq 0.15$ and $\Gamma_1^n \simeq -0.06$ in agreement with recent experiments [5-9], with the Bjørken sum rule being manifestly satisfied.

While our LO analysis was being completed, a full next-to-leading order (NLO) calculation of all polarized two-loop splitting functions $\delta P_{ij}^{(1)}(x)$, $i, j = q, g$, in the conventional $\overline{\text{MS}}$ factorization scheme has appeared for the first time [11]. It is the purpose of this article to present first a consistent NLO formulation of spin-dependent parton distributions, making use of the NLO results of ref.[11], in particular for (Mellin) n -moments of structure functions and parton densities where the solutions of the NLO evolution equations can be obtained analytically. Using these formal results we then proceed to perform a quantitative NLO analysis of $A_1^{p,n}(x, Q^2)$ and $g_1^{p,n}(x, Q^2)$, and will present two sets of NLO $\delta f(x, Q^2)$ for the two scenarios discussed at the beginning. Since most NLO analyses concerning unpolarized hard processes and parton distributions have been performed in the $\overline{\text{MS}}$ factorization scheme, it is convenient to remain within this factorization scheme also for polarized hard processes and spin-dependent parton distributions. This is particularly relevant for the parton distributions which have to satisfy the fundamental positivity constraints (1.3) at any value of x and scale Q^2 , as calculated by the unpolarized and polarized evolution equations, within the *same* factorization scheme. In addition we also repeat our previous LO analysis [1] since new data have been published very recently [6, 7].

2 NLO Parton Distributions and their Q^2 -Evolution

Measurements of polarized deep inelastic lepton nucleon scattering yield direct information [3-9,12] on the spin-asymmetry

$$A_1^N(x, Q^2) \simeq \frac{g_1^N(x, Q^2)}{F_1^N(x, Q^2)} = \frac{g_1^N(x, Q^2)}{F_2^N(x, Q^2)/[2x(1 + R^N(x, Q^2))]} \quad , \quad (2.1)$$

$N = p, n$ and $d = (p+n)/2$, where in the latter case we have used $g_1^d = \frac{1}{2}(g_1^p + g_1^n)(1 - \frac{3}{2}\omega_D)$ with $\omega_D = 0.058$ [7, 9]; $R \equiv F_L/2xF_1 = (F_2 - 2xF_1)/2xF_1$ and subdominant contributions have, as usual, been neglected. In NLO, $A_1^N(x, Q^2)$ is related to the polarized (δf^N) and unpolarized (f^N) quark and gluon distributions in the following way:

$$g_1^N(x, Q^2) = \frac{1}{2} \sum_q e_q^2 \left\{ \delta q^N(x, Q^2) + \delta \bar{q}^N(x, Q^2) + \frac{\alpha_s(Q^2)}{2\pi} \left[\delta C_q * (\delta q^N + \delta \bar{q}^N) + \frac{1}{f} \delta C_g * \delta g \right] \right\} \quad (2.2)$$

with the convolutions being defined by

$$(C * q)(x, Q^2) = \int_x^1 \frac{dy}{y} C\left(\frac{x}{y}\right) q(y, Q^2) \quad (2.3)$$

and where the appropriate spin-dependent Wilson coefficients in the $\overline{\text{MS}}$ scheme are given by (see [11], for example, and references therein)

$$\delta C_q(x) = C_F \left[(1+x^2) \left(\frac{\ln(1-x)}{1-x} \right)_+ - \frac{3}{2} \frac{1}{(1-x)_+} - \frac{1+x^2}{1-x} \ln x + 2 + x - \left(\frac{9}{2} + \frac{\pi^2}{3} \right) \delta(1-x) \right] \quad (2.4)$$

$$\delta C_g(x) = 2T_f \left[(2x-1) \left(\ln \frac{1-x}{x} - 1 \right) + 2(1-x) \right] \quad (2.5)$$

with $C_F = 4/3$ and $T_f = f/2$. Here f denotes, as usual, the number of active flavors ($f = 3$). The NLO expression for the unpolarized (spin-averaged) structure function $F_1^N(x, Q^2)$ is similar to the one in (2.2) with $\delta f(x, Q^2) \rightarrow f(x, Q^2)$ and the unpolarized Wilson coefficients are given, for example, in [13]. Henceforth we shall, as always, use the notation $\delta q^p \equiv \delta q$ and $q^p \equiv q$. Furthermore the NLO running coupling is given by

$$\frac{\alpha_s(Q^2)}{4\pi} \simeq \frac{1}{\beta_0 \ln Q^2 / \Lambda_{\overline{\text{MS}}}^2} - \frac{\beta_1}{\beta_0^3} \frac{\ln \ln Q^2 / \Lambda_{\overline{\text{MS}}}^2}{\left(\ln Q^2 / \Lambda_{\overline{\text{MS}}}^2 \right)^2} \quad (2.6)$$

with $\beta_0 = 11 - 2f/3$, $\beta_1 = 102 - 38f/3$ and $\Lambda_{\overline{\text{MS}}}^{(f)}$ being given by [14]

$$\Lambda_{\overline{\text{MS}}}^{(3,4,5)} = 248, 200, 131 \text{ MeV} \quad .$$

The number of active flavors f in $\alpha_s(Q^2)$ was fixed by the number of quarks with $m_q^2 \leq Q^2$ taking $m_c = 1.5 \text{ GeV}$ and $m_b = 4.5 \text{ GeV}$. The marginal charm contribution to g_1^N ,

stemming from the subprocess $\gamma^*g \rightarrow c\bar{c}$ [15], will be disregarded throughout. The charm contribution to F_1^N is also small in the kinematic range covered by present polarization experiments.

For calculating the NLO evolutions of the spin-dependent parton distributions $\delta f(x, Q^2)$ in (2.2) we have used the well known analytic NLO solutions in Mellin n -moment space (see, e.g., refs.[13, 16, 17]) with the n -th moment being defined by

$$\delta f^n(Q^2) = \int_0^1 dx x^{n-1} \delta f(x, Q^2) \quad . \quad (2.7)$$

These Q^2 -evolutions are governed by the anomalous dimensions¹

$$\delta\gamma_{NS}^n = \frac{\alpha_s}{4\pi} \delta\gamma_{qq}^{(0)n} + \left(\frac{\alpha_s}{4\pi}\right)^2 \delta\gamma_{NS}^{(1)n}(\eta) \quad , \quad \eta = \pm 1 \quad (2.8)$$

$$\delta\gamma_{ij}^n = \frac{\alpha_s}{4\pi} \delta\gamma_{ij}^{(0)n} + \left(\frac{\alpha_s}{4\pi}\right)^2 \delta\gamma_{ij}^{(1)n} \quad , \quad i, j = q, g \quad (2.9)$$

whose detailed n -dependence will be specified in the Appendix. The non-singlet (NS) parton densities evolve according to [13, 16]

$$\delta q_{NS\eta}^n(Q^2) = \left[1 + \frac{\alpha_s(Q^2) - \alpha_s(Q_0^2)}{4\pi} \left(\frac{\delta\gamma_{NS}^{(1)n}(\eta)}{2\beta_0} - \frac{\beta_1 \delta\gamma_{qq}^{(0)n}}{2\beta_0^2} \right) \right] \left(\frac{\alpha_s(Q^2)}{\alpha_s(Q_0^2)} \right)^{\delta\gamma_{qq}^{(0)n}/2\beta_0} \delta q_{NS\eta}^n(Q_0^2) \quad (2.10)$$

with the input scale $Q_0^2 = \mu_{NLO}^2 = 0.34 \text{ GeV}^2$ referring to the radiative [14] NLO input ($\mu_{NLO} = \mu_{HO}$) to be discussed later. Furthermore, opposite to the situation of unpolarized (spin-averaged) parton distributions [16], $\delta q_{NS\eta=+1}$ corresponds to the NS combinations $\delta u - \delta\bar{u} \equiv \delta u_V$ and $\delta d - \delta\bar{d} \equiv \delta d_V$, while $\delta q_{NS\eta=-1}$ corresponds to the combinations $\delta q + \delta\bar{q}$ appearing in the NS expressions

$$\delta q_3 \equiv (\delta u + \delta\bar{u}) - (\delta d + \delta\bar{d}) \quad , \quad \delta q_8 \equiv (\delta u + \delta\bar{u}) + (\delta d + \delta\bar{d}) - 2(\delta s + \delta\bar{s}) \quad . \quad (2.11)$$

It should be noted that the first ($n = 1$) moments $\delta q_{NS-}^1 \equiv \Delta q_{NS-}$ of these latter $SU(3)_f$ diagonal flavor non-singlet combinations do *not* renormalize, i.e. are independent of Q^2 , due to the conservation of the flavor non-singlet axial vector current, i.e.

¹ Alternatively one can of course use instead the LO and NLO splitting functions $\delta P_{ij}^{(0)n} = -\delta\gamma_{ij}^{(0)n}/4$ and $\delta P_{ij}^{(1)n} = -\delta\gamma_{ij}^{(1)n}/8$, respectively (see, e.g., ref.[17]).

$\delta\gamma_{qq}^{(0)1} = \delta\gamma_{NS}^{(1)1}(\eta = -1) = 0$ (see Appendix). The evolution in the flavor singlet sector, i.e. of

$$\delta\Sigma^n(Q^2) \equiv \sum_{q=u,d,s} [\delta q^n(Q^2) + \delta\bar{q}^n(Q^2)] \quad (2.12)$$

and $\delta g^n(Q^2)$ is governed by the anomalous dimension 2×2 matrix (2.9) with the explicit solution given by eq.(2.9) of ref.[16] where $\gamma \rightarrow \delta\gamma$ as given in the Appendix.

Having obtained the analytic NLO solutions for the moments of parton densities, $\delta f^n(Q^2)$, it is simple to (numerically) Mellin-invert them to Björken- x space as described, for example, in [16] or [17]. The so obtained $\delta f(x, Q^2)$ have to be convoluted with the Wilson coefficients in (2.2) to yield the desired $g_1(x, Q^2)$. Alternatively, one could insert $\delta f^n(Q^2)$ directly into the n -th moment of eq.(2.2),

$$g_1^n(Q^2) = \frac{1}{2} \sum_q e_q^2 \left\{ \delta q^n(Q^2) + \delta\bar{q}^n(Q^2) + \frac{\alpha_s(Q^2)}{2\pi} \left[\delta C_q^n (\delta q^n(Q^2) + \delta\bar{q}^n(Q^2)) + \frac{1}{f} \delta C_g^n \delta g^n(Q^2) \right] \right\} \quad (2.2')$$

with the moments of (2.4) and (2.5) given by

$$\delta C_q^n = C_F \left[-S_2(n) + (S_1(n))^2 + \left(\frac{3}{2} - \frac{1}{n(n+1)} \right) S_1(n) + \frac{1}{n^2} + \frac{1}{2n} + \frac{1}{n+1} - \frac{9}{2} \right] \quad (2.4')$$

$$\delta C_g^n = 2T_f \left[-\frac{n-1}{n(n+1)} (S_1(n) + 1) - \frac{1}{n^2} + \frac{2}{n(n+1)} \right] \quad (2.5')$$

with $S_k(n)$ defined in the Appendix. The full expression (2.2') can now be directly (numerically) Mellin-inverted [16, 17] to yield $g_1(x, Q^2)$ without having to calculate any convolution (2.3).

The LO results are of course entailed in all these expressions given above, by simply dropping all the obvious higher order terms (β_1 , $\delta\gamma^{(1)}$, $\delta C_{q,g}$) in all relevant equations stated above.

It should be noted that the first ($n = 1$) moment $\Gamma_1(Q^2) \equiv g_1^1(Q^2)$ in (1.5) is, according to (2.2'), simply given by

$$\Gamma_1(Q^2) = \frac{1}{2} \sum_q e_q^2 \left(1 - \frac{\alpha_s(Q^2)}{\pi} \right) [\Delta q(Q^2) + \Delta\bar{q}(Q^2)] \quad (2.13)$$

where we have used the definition (1.1) and $\delta C_q^1 = -3C_F/2$ and $\delta C_g^1 = 0$ according to (2.4') and (2.5'), respectively. Thus, the total gluon helicity $\Delta g(Q^2)$ does not directly couple to $\Gamma_1(Q^2)$ due to the vanishing of the integrated gluonic coefficient function in the $\overline{\text{MS}}$ factorization scheme. This vanishing of $\Delta C_g \equiv \delta C_g^1$, which has been some matter of dispute during the past years (for reviews see, for example, [12, 18, 19]) originates from the last term in (2.5) proportional to $2(1-x)$. Since this term derives from the soft non-perturbative collinear region [20] where $k_T^2 \sim m_q^2 \ll \Lambda^2$, it has been suggested [18, 21-23] to absorb it into the definition of the light (non-perturbative) input (anti)quark distributions $\delta q^{(-)}(x, Q^2 = Q_0^2)$. This implies that, instead of $\delta C_g(x)$ in (2.5), one has

$$\delta \tilde{C}_g(x) = 2T_f(2x-1) \left(\ln \frac{1-x}{x} - 1 \right) \quad (2.14)$$

which refers to some different factorization scheme [18, 22, 23] with the n -th moment given by

$$\delta \tilde{C}_g^n = \delta C_g^n - 2T_f \frac{2}{n(n+1)} \quad (2.14')$$

and δC_g^n given in (2.5'). Thus $\Delta \tilde{C}_g \equiv \delta \tilde{C}_g^1 = -2T_f$ and $\Delta g(Q^2)$ would couple directly [21] to $\Gamma_1(Q^2)$ in (2.13) via $-(\alpha_s/6\pi)\Delta g(Q^2)$ according to the gluonic term in the curly brackets of (2.2') for $f = 3$ flavors. Therefore the gluonic contribution on its own could account for a reduction [18, 21, 22] of the Ellis-Jaffe estimate (1.4), as required by experiment, without the need of a sizeable negative total (strange) sea helicity as discussed in the Introduction. One could of course choose to work within this particular factorization scheme or any other scheme. In this case, however, one has for consistency reasons to calculate *all* polarized NLO quantities ($\delta C_i^n, \delta \gamma_{ij}^{(1)n}$, etc.), and not just their first ($n = 1$) moments, in these specific schemes *as well as* also NLO subprocesses of purely hadronic reactions to which the NLO parton distributions are applied to. The transformation² $\delta C_g^n \rightarrow \delta \tilde{C}_g^n$ in (2.14') implies of course also a corresponding modification [13, 24] of the NLO anomalous dimensions $\delta \gamma_{ij}^{(1)n} \rightarrow \delta \tilde{\gamma}_{ij}^{(1)n}$.

² This transformation cannot even be uniquely defined for the spin dependent case. This is partly in contrast to the unpolarized situation [13, 24, 16] where the energy-momentum conservation constraint (for $n = 2$) is used together with the assumption of its analyticity in n .

3 Quantitative NLO Analysis

In fixing the polarized NLO input parton distributions $\delta f(x, Q^2 = \mu_{NLO}^2)$ we follow closely our recent LO analysis [1]. We still prefer to work with the directly measured asymmetry $A_1^N(x, Q^2)$ in (2.1), rather than with the derived $g_1^N(x, Q^2)$, since possible non-perturbative (higher twist) contributions are expected to partly cancel in the ratio of structure functions appearing in $A_1^N(x, Q^2)$, in contrast to the situation for $g_1^N(x, Q^2)$. Therefore we shall use all presently available data [4-9] in the small- x region where $Q^2 \gtrsim 1 \text{ GeV}^2$ without bothering about lower cuts in Q^2 usually introduced in order to avoid possible higher twist effects as mandatory for analyzing $g_1^N(x, Q^2)$ in the low- Q^2 region. The analysis affords some well established set of unpolarized NLO parton distributions $f(x, Q^2)$ for calculating $F_1^N(x, Q^2)$ in (2.1) which will be adopted from ref.[14], i.e. our recent updated NLO ($\overline{\text{MS}}$) dynamical distributions valid down to the radiative input scale $Q^2 = \mu_{NLO}^2 = 0.34 \text{ GeV}^2$.

The searched for polarized NLO (as well as LO) parton distributions $\delta f(x, Q^2)$, compatible with present data [4-9] on $A_1^N(x, Q^2)$, are constrained by the positivity requirements (1.3) and for the $SU(3)_f$ symmetric 'standard' scenario by the sum rules

$$\Delta u + \Delta \bar{u} - \Delta d - \Delta \bar{d} = g_A = F + D = 1.2573 \pm 0.0028 \quad (3.1)$$

$$\Delta u + \Delta \bar{u} + \Delta d + \Delta \bar{d} - 2(\Delta s + \Delta \bar{s}) = 3F - D = 0.579 \pm 0.025 \quad (3.2)$$

with the first moment Δf defined in (1.1) and the values of g_A and $3F - D$ taken from [25]. It should be remembered that the first moments $\Delta q_{3,8}$ of the flavor non-singlet combinations (2.11) which appear in (3.1) and (3.2) are Q^2 -independent also in NLO due to $\delta\gamma_{NS}^{(1)1}(\eta = -1) = 0$, according to eq.(A.9).

As a plausible alternative to the full $SU(3)_f$ symmetry between charged weak and neutral axial currents required for deriving the 'standard' constraints (3.1) and (3.2), we consider a 'valence' scenario [1, 2] where this flavor symmetry is broken and which is based on the assumption [2] that the flavor changing hyperon β -decay data fix only the total helicity of *valence* quarks $\Delta q_V(Q^2) \equiv \Delta q - \Delta \bar{q}$:

$$\Delta u_V(\mu_{NLO}^2) - \Delta d_V(\mu_{NLO}^2) = g_A = F + D = 1.2573 \pm 0.0028 \quad (3.1')$$

$$\Delta u_V(\mu_{NLO}^2) + \Delta d_V(\mu_{NLO}^2) = 3F - D = 0.579 \pm 0.025 \quad . \quad (3.2')$$

Although at the input scale $\Delta\bar{u}(\mu_{NLO}^2) = \Delta\bar{d}(\mu_{NLO}^2)$, isospin symmetry will be (marginally) broken by the NLO evolution, i.e. $\Delta\bar{u}(Q^2) \neq \Delta\bar{d}(Q^2)$ for $Q^2 > \mu_{NLO}^2$. In addition we shall assume a maximally $SU(3)_f$ broken polarized strange sea input $\delta s(x, \mu_{NLO}^2) = \delta\bar{s}(x, \mu_{NLO}^2) = 0$ in our 'valence' scenario, which in addition is compatible with the $SU(3)_f$ broken unpolarized radiative input $s(x, \mu_{NLO}^2) = 0$ of ref.[14]. Such a choice is feasible in the 'valence' scenario since, due to eq.(2.13) and (2.11), we have in general

$$\Gamma_1^{p,n}(Q^2) = \left[\pm \frac{1}{12} \Delta q_3 + \frac{1}{36} \Delta q_8 + \frac{1}{9} \Delta \Sigma(Q^2) \right] \left(1 - \frac{\alpha_s(Q^2)}{\pi} \right) \quad . \quad (3.3)$$

Since $\Delta u_V(Q^2) - \Delta d_V(Q^2)$ and $\Delta u_V(Q^2) + \Delta d_V(Q^2)$ decrease only marginally with Q^2 as compared to their input values in (3.1') and (3.2') [cf. Table 1' below], and furthermore the dynamical isospin breaking $\Delta\bar{u} \neq \Delta\bar{d}$ at $Q^2 > \mu_{NLO}^2$ is small, eq.(3.3) can be approximated by

$$\Gamma_1^{p,n}(Q^2) \simeq \left[\pm \frac{1}{12} (F + D) + \frac{5}{36} (3F - D) + \frac{1}{18} (10\Delta\bar{q}(Q^2) + \Delta s(Q^2) + \Delta\bar{s}(Q^2)) \right] \left(1 - \frac{\alpha_s(Q^2)}{\pi} \right) \quad . \quad (3.4)$$

Therefore a light polarized sea $\Delta\bar{q} \equiv (\Delta\bar{u} + \Delta\bar{d})/2 < 0$ can account for the reduction of the Ellis-Jaffe estimate (1.4) for $\Gamma_1^p(Q^2)$, say, as required by recent experiments [5, 6].

In the 'standard' scenario we need, on the contrary, a finite sizeable $\Delta s(Q^2) < 0$ since, due to eq.(2.13) and (2.11),

$$\Gamma_1^{p,n}(Q^2) = \left[\pm \frac{1}{12} \Delta q_3 + \frac{5}{36} \Delta q_8 + \frac{1}{3} (\Delta s(Q^2) + \Delta\bar{s}(Q^2)) \right] \left(1 - \frac{\alpha_s(Q^2)}{\pi} \right) \quad (3.5)$$

with the Q^2 -independent flavor non-singlet combinations $\Delta q_{3,8}$ being entirely fixed by eqs.(3.1) and (3.2); for the singlet combination in (1.2) we used $\Delta \Sigma(Q^2) = \Delta q_8 + 3(\Delta s(Q^2) + \Delta\bar{s}(Q^2))$. It should be noted that, in contrast to the LO [1] case, a finite $\Delta s(Q^2)$ will be generated dynamically in NLO for $Q^2 > \mu_{NLO}^2$ even for a vanishing input $\Delta s(\mu_{NLO}^2) = 0$ due to the non-vanishing NLO $\Delta\gamma_{qq}^{(1)}$ in (A.9): The resulting 'dynamical' $\Delta s(Q^2) < 0$ is about an order of magnitude too small to comply with recent experiments [5, 6] which typically yield, for example, $\Gamma_1^p(Q^2 = 3 \text{ GeV}^2) \simeq 0.12 - 0.13$, i.e. sizeably

smaller than the naive estimate (1.4). We therefore have to implement a *finite* strange sea input $\Delta s(\mu_{NLO}^2) = \Delta \bar{s}(\mu_{NLO}^2) < 0$ for the 'standard' scenario, in order to arrive at $\Delta s(Q^2 = 3 - 10 \text{ GeV}^2) \simeq -0.05$ as required [1] by recent experiments.

Apart from applying the above scenarios for the polarized input distributions to $A_1^N(x, Q^2)$ rather than to $g_1^N(x, Q^2)$, the main ingredient of our NLO analysis is the implementation of the positivity constraints (1.3) down to [14] $Q^2 = \mu_{NLO}^2 = 0.34 \text{ GeV}^2$ (and to $Q^2 = \mu_{LO}^2 = 0.23 \text{ GeV}^2$ in LO) which is not guaranteed in the usual (LO) studies done so far (recently, e.g., in [26-29]) restricted to $Q^2 \geq Q_0^2 = 1 - 4 \text{ GeV}^2$. We follow here the radiative (dynamical) concept which resulted in the successful small- x predictions of unpolarized parton distributions as measured at HERA [14, 16, 30]. A further advantage of this analysis is the possibility to study the Q^2 -dependence of $A_1^N(x, Q^2)$ in the small- x region over a wide range of Q^2 [6] which might be also relevant for the forthcoming polarized experiments at HERA. In addition it will be important to learn about the reliability of perturbative calculations by comparing the LO with the NLO results; a reasonable perturbative stability of all radiative model predictions will be indeed observed for *measurable* quantities such as $A_1^N(x, Q^2)$ and $g_1^N(x, Q^2)$, as is the case for spin-averaged deep inelastic structure functions [14, 30].

Turning to the determination of the polarized NLO (LO) parton distributions $\delta f(x, Q^2)$ it is helpful to consider some reasonable theoretical constraints concerning the sea and gluon distributions, in particular in the relevant small- x region where only rather scarce data exist at present, such as color coherence of gluon couplings at $x \simeq 0$ and helicity retention properties of valence densities as $x \rightarrow 1$ [31]. We follow here very closely the procedure and ansätze of ref.[1]. Subject to these constraints we employ the following general ansatz for the NLO (LO) polarized parton distributions:

$$\begin{aligned}
\delta q_V(x, \mu^2) &= N_{q_V} x^{a_{q_V}} q_V(x, \mu^2) \\
\delta \bar{q}(x, \mu^2) &= N_{\bar{q}} x^{a_{\bar{q}}} (1-x)^{b_{\bar{q}}} \bar{q}(x, \mu^2) \\
\delta s(x, \mu^2) &= \delta \bar{s}(x, \mu^2) = N_s \delta \bar{q}(x, \mu^2) \\
\delta g(x, \mu^2) &= N_g x^{a_g} (1-x)^{b_g} g(x, \mu^2)
\end{aligned} \tag{3.6}$$

with the NLO (LO) unpolarized input densities being taken from ref.[14] and, for obvious

reasons, we have not taken into account any $SU(2)_f$ breaking input ($\delta\bar{u} \neq \delta\bar{d}$) as is apparent from our ansatz for $\delta\bar{q} \equiv \delta\bar{u} \equiv \delta\bar{d}$ proportional to $\bar{q} \equiv (\bar{u} + \bar{d})/2$ which should be considered as the reference light sea distribution for the positivity requirement (1.3). In the ‘standard’ scenario our optimal NLO densities at $Q^2 = \mu_{NLO}^2 = 0.34 \text{ GeV}^2$ are given by

$$\begin{aligned}
N_{u_V} &= 0.6586 \quad , \quad a_{u_V} = 0.18 \quad ; \quad N_{d_V} = -0.3392 \quad , \quad a_{d_V} = 0 \\
N_{\bar{q}} &= -0.525 \quad , \quad a_{\bar{q}} = 0.51 \quad , \quad b_{\bar{q}} = 0 \quad ; \quad N_s = 1 \\
N_g &= 10.47 \quad , \quad a_g = 1.1 \quad , \quad b_g = 4.3
\end{aligned} \tag{3.7}$$

corresponding to $\chi^2 = 104.5/125$ d.o.f. and respecting eqs.(3.1) and (3.2) which are the basis of almost all analyses performed so far.^{3,4} Since new polarized p and d data have appeared very recently [6, 7], we have also again determined the LO distributions in the ‘standard’ scenario at $Q^2 = \mu_{LO}^2 = 0.23 \text{ GeV}^2$:

$$\begin{aligned}
N_{u_V} &= 0.6392 \quad , \quad a_{u_V} = 0.16 \quad ; \quad N_{d_V} = -0.3392 \quad , \quad a_{d_V} = 0 \\
N_{\bar{q}} &= -1.348 \quad , \quad a_{\bar{q}} = 0.93 \quad , \quad b_{\bar{q}} = 0.09 \quad ; \quad N_s = 1 \\
N_g &= 11.8 \quad , \quad a_g = 0.76 \quad , \quad b_g = 6.84
\end{aligned} \tag{3.7'}$$

corresponding to $\chi^2 = 108.0/125$ d.o.f. and which supercedes our LO input fit of ref.[1]. The fact that $\delta s(x, \mu^2) \neq 0$ in (3.7) and (3.7'), i.e. $N_s = 1$, contradicts somewhat our purely radiative input [14] $s(x, \mu^2) = \bar{s}(x, \mu^2) = 0$, but for $Q^2 \gtrsim 1 \text{ GeV}^2$ the positivity inequality (1.3) is already satisfied, in particular at large values of x . In this respect the input for the ‘valence’ scenario with the extreme $SU(3)_f$ breaking ansatz $\delta s(x, \mu^2) = 0$ is more consistent as far as our radiative (dynamical) approach is concerned: For the $SU(3)_f$ broken ‘valence’ scenario, based on the constraints (3.1') and (3.2'), our optimal

³ It is interesting to note that, within our radiative approach with its longer Q^2 -evolution ‘distance’, a *finite* (negative) strange sea input $\delta s(x, \mu_{NLO}^2)$ is *always* required by present data even if one uses $\delta\tilde{C}_g$ in (2.14) or (2.14') [21-23]. For the latter case, δs has to be at least half as large as in (3.5) which is based on the $\overline{\text{MS}}$ δC_g in (2.5) or (2.5'). This holds true even for a maximally saturated input gluon [$\delta g(x, \mu_{NLO}^2) = g(x, \mu_{NLO}^2)$] to be discussed below.

⁴ It should be noted that our fit result $N_s = 1$ in (3.7) implies via (3.6) an $SU(3)_f$ symmetric sea input. In NLO at $Q^2 > \mu_{NLO}^2$ this symmetry becomes dynamically broken via the Q^2 -evolution. In view of present scarce data such $SU(3)_f$ [and $SU(2)_f$] breaking effects are entirely negligible for quantitative analyses.

NLO input corresponds to the following parameters in (3.6) at $\mu_{NLO}^2 = 0.34 \text{ GeV}^2$:

$$\begin{aligned}
N_{u_V} &= 0.6708 , \quad a_{u_V} = 0.19 ; \quad N_{d_V} = -0.3693 , \quad a_{d_V} = 0.03 \\
N_{\bar{q}} &= -0.6 , \quad a_{\bar{q}} = 0.5 , \quad b_{\bar{q}} = 0 ; \quad N_s = 0 \\
N_g &= 9.87 , \quad a_g = 1.05 , \quad b_g = 4.44
\end{aligned} \tag{3.8}$$

corresponding to $\chi^2 = 104.6/125$ d.o.f. Similarly our new LO input at $\mu_{LO}^2 = 0.23 \text{ GeV}^2$ in the 'valence' scenario is given by

$$\begin{aligned}
N_{u_V} &= 0.6272 , \quad a_{u_V} = 0.15 ; \quad N_{d_V} = -0.3392 , \quad a_{d_V} = 0 \\
N_{\bar{q}} &= -1.455 , \quad a_{\bar{q}} = 0.88 , \quad b_{\bar{q}} = 0.13 ; \quad N_s = 0 \\
N_g &= 7.4 , \quad a_g = 0.6 , \quad b_g = 5.93
\end{aligned} \tag{3.8'}$$

corresponding to $\chi^2 = 108.6/125$ d.o.f. and which supercedes our LO input fit of ref.[1]. Finally, similarly agreeable NLO 'valence' scenario fits to all present asymmetry data shown below (with a total χ^2 of 106.2 to 107.6 for 125 data points) can be also obtained for a fully saturated (inequality (1.3)) gluon input $\delta g(x, \mu_{NLO}^2) = g(x, \mu_{NLO}^2)$ as well as for the less saturated $\delta g(x, \mu_{NLO}^2) = xg(x, \mu_{NLO}^2)$. A purely dynamical [32] input $\delta g(x, \mu_{NLO}^2) = 0$ is also compatible with present data, but such a choice seems to be unlikely in view of $\delta \bar{q}(x, \mu_{NLO}^2) \neq 0$; it furthermore results in an unphysically steep [32] $\delta g(x, Q^2 > \mu_{NLO}^2)$, being mainly concentrated in the very small- x region $x < 0.01$, as in the corresponding case [16, 33] for the unpolarized parton distributions in disagreement with experiment. Similar remarks hold also for a LO analysis as well as for the 'standard' scenario.

A comparison of our results with the data on $A_1^N(x, Q^2)$ is presented in Fig.1. The LO and NLO results in the 'standard' scenario are perturbatively stable and almost indistinguishable. The same holds true for the results in the 'valence' scenario which are not shown separately since they almost coincide with the 'standard' ones in Fig.1. As already mentioned, fit results using a 'saturated' gluon $\delta g = g$ or $\delta g = xg$, or even $\delta g = 0$ at $Q^2 = \mu_{LO, NLO}^2$ are very similar to the ones shown in Fig.1. Note that $A_1^N(x, Q^2) \rightarrow \text{const.}$ as $x \rightarrow 1$. The recently measured Q^2 - dependence of $A_1^N(x, Q^2)$ [6] is compared with our theoretical results down to $Q^2 = 0.4 \text{ GeV}^2$ in Fig.2. The difference between our LO and NLO results in the small- Q^2 region is mainly due to different LO ($\mu_{LO}^2 = 0.23 \text{ GeV}^2$) and

NLO ($\mu_{NLO}^2 = 0.34 \text{ GeV}^2$) input scales. The more detailed Q^2 -dependence of $A_1^N(x, Q^2)$ is presented in Fig.3 for some typical fixed x values for $1 \lesssim Q^2 \leq 20 \text{ GeV}^2$ relevant for present experiments. The predicted scale-violating NLO Q^2 -dependence is similar to the LO one; for $x > 0.01$ this is also the case for the two rather different input scenarios (3.1), (3.2) and (3.1'), (3.2'). In the (x, Q^2) region of present data [4-9], $A_1^p(x, Q^2)$ increases with Q^2 for $x > 0.01$. Therefore, since most present data in the small- x region correspond to small values of $Q^2 \gtrsim 0.5 \text{ GeV}^2$, the determination of $g_1^p(x, Q^2)$ at a larger fixed Q^2 (5 or 10 GeV^2 , say) by assuming $A_1^p(x, Q^2)$ to be independent of Q^2 , as is commonly done [4-9] (except for the recent last reference of [6]), is misleading and might lead to an *underestimate* of g_1^p by as much as about 20%, in particular in the small- x region $x \gtrsim 0.02$. (For $x \lesssim 0.01$ the effect will be opposite.) The situation is opposite, although less pronounced, for $-A_1^n(x, Q^2)$ shown in Fig.3. This implies that $|g_1^n(x, Q^2)|$ might be *overestimated* at larger fixed Q^2 by assuming $A_1^n(x, Q^2)$, as measured at small Q^2 , to be independent of Q^2 . It is obvious that the assumption of approximate scaling for $A_1(x, Q^2)$ is therefore unwarranted and, in any case, theoretically not justified as soon as gluon and sea densities become relevant, due to the very different polarized and unpolarized splitting functions (anomalous dimensions) in the flavor singlet sector.

In Fig.4 we compare our NLO results for $g_1^N(x, Q^2)$ with EMC, SMC and SLAC-E142/E143 data as well as with our LO results which are similar to our original LO results [1]. The reason why the LO results are partly larger by more than about 10% than the NLO ones is mainly due to the LO approximation where $R^N = 0$ in (2.1). Although the agreement between the NLO results and experiment has been significantly improved, the EMC [4] and E143 [6] 'data' at fixed values of Q^2 fall still below our NLO predictions in the small- x region. This is partly due to the fact that the original small- x A_1^p -data at small Q^2 have been extrapolated [4, 6] to a larger fixed value of Q^2 by assuming $A_1^p(x, Q^2)$ to be independent of Q^2 . According to the increase of A_1^p with Q^2 in Fig.3, such an assumption underestimates g_1^p in the small- x region at larger Q^2 . On the contrary, our results for $g_1^{p,d}$ do not show such a disagreement in the small- x region when compared with the SMC data [5, 7] in Figs. 4a and 4b where each data point corresponds to a different value of Q^2 since no attempt has been made to extrapolate $g_1^N(x, Q^2)$ to a fixed Q^2 from

the originally measured $A_1^N(x, Q^2)$. Our predictions for the NLO parton distributions at the input scale $Q^2 = \mu_{NLO}^2$ in eq.(3.6) with the fit parameters given in (3.7) and (3.8) are shown in Fig.5a; the corresponding LO inputs at $Q^2 = \mu_{LO}^2$ in eq.(3.6) with the fit parameters given in (3.7') and (3.8') are shown in Fig.5b. The polarized input densities in Figs. 5a and 5b are compared with our reference unpolarized NLO and LO dynamical input densities of ref.[14] which satisfy of course the positivity requirement (1.3) as is obvious from eq.(3.6). The distributions at $Q^2 = 4 \text{ GeV}^2$, as obtained from these inputs at $Q^2 = \mu^2$ for the two scenarios considered, are shown in Fig.6. Since not even the polarized NLO gluon density $\delta g(x, Q^2)$ is strongly constrained by present experiments, we compare our gluons at $Q^2 = 4 \text{ GeV}^2$ in Fig.7 with the ones which originate from imposing extreme inputs at $Q_0^2 = \mu_{NLO}^2$, such as $\delta g = g$, $\delta g = xg$ and $\delta g = 0$, instead of the one in (3.6) for the 'valence' scenario. The results are similar if these extreme gluon-inputs are taken for the 'standard' scenario in (3.6), and the variation of $\delta g(x, Q^2)$ allowed by present experiments is indeed sizeable. This implies, in particular, that the Q^2 -evolution of $g_1(x, Q^2)$ below the experimentally accessible x -range is *not* predictable for the time being.

Finally let us turn to the first moments (total polarizations) $\Delta f(Q^2)$ of our polarized parton distributions, as defined in (1.1), and the resulting $\Gamma_1^{p,n}(Q^2)$ in (3.3). It should be recalled that, in contrast to the LO, the first moments of the NLO (anti)quark densities do renormalize, i.e. are Q^2 -dependent, due to the non-vanishing of the 2-loop $\delta\gamma_{qq}^{(1)1}$ in (A.9) and $\delta\gamma_{NS}^{(1)1}(\eta = +1)$ in (2.10). Let us discuss the two scenarios in turn:

'standard' scenario: From the input distributions (3.6) together with (3.7), being constrained by (3.1) and (3.2), one infers in NLO

$Q^2 (\text{GeV}^2)$	Δu_V	Δd_V	$\Delta \bar{q}$	$\Delta s = \Delta \bar{s}$	Δg	$\Delta \Sigma$	Γ_1^p	Γ_1^n
μ_{NLO}^2	0.9181	-0.3392	-0.0660	-0.0660	0.507	0.183	0.1136	-0.0550
1	0.915	-0.338	-0.067	-0.068	0.961	0.173	0.124	-0.061
4	0.914	-0.338	-0.068	-0.068	1.443	0.168	0.128	-0.064
10	0.914	-0.338	-0.068	-0.069	1.737	0.166	0.130	-0.065

Table 1. First moments Δf of polarized NLO parton densities $\delta f(x, Q^2)$ and of $g_1^{p,n}(x, Q^2)$ as predicted in the 'standard' scenario. Note that the marginal differences for $\Delta\bar{q}$ and Δs indicate the typical amount of dynamical $SU(3)_f$ breaking as mentioned in footnote 4.

In LO the input distributions (3.6) together with (3.7') imply

$$\begin{aligned} \Delta u_V &= 0.9181 \quad , \quad \Delta d_V = -0.3392 \quad , \quad \Delta\bar{q} = \Delta s = \Delta\bar{s} = -0.0587 \quad , \\ \Delta g(\mu_{LO}^2) &= 0.362 \quad , \quad \Delta g(4 \text{ GeV}^2) = 1.273 \quad , \quad \Delta g(10 \text{ GeV}^2) = 1.570 \end{aligned} \quad (3.9)$$

which result in $\Delta\Sigma = 0.227$. This gives, using eq.(3.5) without the factor α_s/π together with (3.1) and (3.2),

$$\Gamma_1^p = 0.1461 \quad , \quad \Gamma_1^n = -0.0635 \quad (3.10)$$

which is similar to our previous LO result [1]. Both our NLO results in Table 1 and the LO ones in (3.10) are in satisfactory agreement with recent SMC and EMC measurements [4, 5, 7]

$$\Gamma_1^p(10 \text{ GeV}^2) = 0.142 \pm 0.008 \pm 0.011, \quad \Gamma_1^n(10 \text{ GeV}^2) = -0.063 \pm 0.024 \pm 0.013 \quad (3.11)$$

as well as with the most recent E143 data [9] implying $\Gamma_1^n(2 \text{ GeV}^2) = -0.037 \pm 0.008 \pm 0.011$.

'valence' scenario: From the input distributions (3.6) together with (3.8), being constrained by (3.1') and (3.2'), one infers in NLO

Q^2 (GeV ²)	Δu_V	Δd_V	$\Delta\bar{q}$	$\Delta s = \Delta\bar{s}$	Δg	$\Delta\Sigma$	Γ_1^p	Γ_1^n
μ_{NLO}^2	0.9181	-0.3392	-0.0778	0	0.496	0.268	0.1142	-0.0544
1	0.915	-0.338	-0.080	-2.5×10^{-3}	0.982	0.252	0.124	-0.061
4	0.914	-0.338	-0.081	-3.5×10^{-3}	1.494	0.245	0.128	-0.064
10	0.914	-0.338	-0.081	-3.8×10^{-3}	1.807	0.244	0.130	-0.065

Table 1'. First moments Δf of polarized NLO parton densities $\delta f(x, Q^2)$ and of $g_1^{p,n}(x, Q^2)$ as predicted in the 'valence' scenario.

In LO the input distributions (3.6) together with (3.8') imply

$$\begin{aligned} \Delta u_V = 0.9181 \quad , \quad \Delta d_V = -0.3392 \quad , \quad \Delta \bar{q} = -0.0712 \quad , \quad \Delta s = \Delta \bar{s} = 0 \quad , \\ \Delta g(\mu_{LO}^2) = 0.372 \quad , \quad \Delta g(4 \text{ GeV}^2) = 1.361 \quad , \quad \Delta g(10 \text{ GeV}^2) = 1.684 \quad (3.9') \end{aligned}$$

which result in $\Delta\Sigma = 0.294$. This gives, using eq.(3.4) without the factor α_s/π together with (3.1') and (3.2'),

$$\Gamma_1^p = 0.1456 \quad , \quad \Gamma_1^n = -0.0639 \quad (3.10')$$

which is again similar to our previous LO result [1]. Both our NLO results in Table 1' and the LO ones in (3.10') compare again well with the experimental results in (3.11).

Apart from the Q^2 -dependent $\Delta g(Q^2)$ in LO and NLO, the Q^2 -dependent first moments of NLO (anti)quark densities in Table 1 and 1' should be compared with the Q^2 -independent LO results as discussed in the Introduction which, in absolute magnitude, are similar to the NLO ones. Although present scarce data obviously cannot uniquely fix the polarized sea and gluon densities, our optimal fits favor a sizeable total gluon helicity, $\Delta g(10 \text{ GeV}^2) \simeq 1.7$, despite the fact that $\Delta g(Q^2)$ decouples from the full first moment $\Gamma_1(Q^2)$ in (2.13) in the $\overline{\text{MS}}$ scheme.

In both scenarios the Bjørken sum rule manifestly holds in LO due to our constraints (3.1) and (3.1'), and together with the NLO correction due to eq.(3.3) we have

$$\Gamma_1^p(Q^2) - \Gamma_1^n(Q^2) = \frac{1}{6} g_A \left(1 - \frac{\alpha_s(Q^2)}{\pi} \right) \quad . \quad (3.12)$$

It is also interesting to observe that at our low input scales $Q^2 = \mu_{LO,NLO}^2 = 0.23, 0.34 \text{ GeV}^2$ the nucleon's spin is dominantly carried just by the total helicities of quarks and gluons, $\frac{1}{2}\Delta\Sigma(\mu_{NLO}^2) + \Delta g(\mu_{NLO}^2) \simeq 0.6$ according to Tables 1 and 1', and $\frac{1}{2}\Delta\Sigma + \Delta g(\mu_{LO}^2) \simeq 0.5$ according to eqs.(3.9) and (3.9'), which implies for the helicity sum rule

$$\frac{1}{2} = \frac{1}{2}\Delta\Sigma(Q^2) + \Delta g(Q^2) + L_z(Q^2) \quad (3.13)$$

that $L_z(\mu_{LO,NLO}^2) \simeq 0$. The approximate vanishing of the latter non-perturbative angular momentum, being build up from the intrinsic k_T carried by partons, is intuitively expected for low (bound-state-like) scales but not for $Q^2 \gg \mu_{LO,NLO}^2$.

4 Summary

Based on a recent complete NLO calculation [11] of all spin-dependent two-loop splitting functions $\delta P_{ij}^{(1)}(x)$, $i, j = q, g$ (or, equivalently, anomalous dimensions $\delta\gamma_{ij}^{(1)}$) in the conventional $\overline{\text{MS}}$ factorization scheme, we have first presented a consistent NLO formulation of the Q^2 -evolution of polarized parton distributions. For calculational purposes we have concentrated on (Mellin) n -moments of structure functions where the solutions of the NLO evolution equations can be obtained analytically for the parton densities. Using these formal results we have performed a quantitative NLO analysis of the longitudinal spin asymmetry $A_1^{p,n}(x, Q^2)$ and of $g_1^{p,n}(x, Q^2)$, and we have updated our previous LO results [1]. Within the whole relevant x - and Q^2 -region ($x \gtrsim 10^{-3}$, $Q^2 \gtrsim 1 \text{ GeV}^2$) we found a remarkable perturbative stability between LO and NLO results. The scale violating Q^2 -dependence of $A_1^{p,n}(x, Q^2)$ turned out to be similar to the one obtained in LO and is *non-negligible* for (x, Q^2) values relevant for present data. The assumption of approximate scaling for $A_1(x, Q^2)$ is therefore unwarranted and theoretically not justified. We presented two plausible sets of polarized LO and NLO ($\overline{\text{MS}}$) parton densities $\delta f(x, Q^2)$ which describe all presently available data very well. In contrast to polarized quark and antiquark densities, the gluon density $\delta g(x, Q^2)$ is rather weakly constrained by present data. Our optimal fits, however, favor a rather sizeable total gluon helicity, e.g., $\Delta g(Q^2 = 10 \text{ GeV}^2) \simeq 1.7$. It should be reemphasized that only processes where δg occurs *directly* already in LO (with no δq and $\delta\bar{q}$ contributions present) appear to be the most promising sources for measuring $\delta g(x, Q^2)$. This is the case for $\gamma^*(\gamma)\delta g \rightarrow c\bar{c}$ responsible for open charm or J/Ψ production (see, e.g., ref.[15]). Our results demonstrate the compatibility of our restrictive radiative model, cf. eq.(1.3), down to $Q^2 = \mu_{NLO}^2 = 0.34 \text{ GeV}^2$ and to $Q^2 = \mu_{LO}^2 = 0.23 \text{ GeV}^2$, with present measurements of deep inelastic spin asymmetries and structure functions.

A FORTRAN package containing our optimally fitted 'standard' and 'valence' NLO ($\overline{\text{MS}}$) as well as LO distributions can be obtained by electronic mail from stratmann@het.physik.uni-dortmund.de or vogelsang@v2.rl.ac.uk.

Acknowledgements

We are grateful to Willy van Neerven for helpful discussions about the complete NLO($\overline{\text{MS}}$) calculation of the spin-dependent splitting functions. This work has been supported in part by the 'Bundesministerium für Bildung, Wissenschaft, Forschung und Technologie', Bonn.

Appendix

The spin-dependent LO anomalous dimensions (splitting functions¹) have been originally calculated in [34, 35] and are given by

$$\begin{aligned}
 \delta\gamma_{qq}^{(0)n} &= 4C_F \left[2S_1(n) - \frac{1}{n(n+1)} - \frac{3}{2} \right] \\
 \delta\gamma_{qg}^{(0)n} &= -8T_f \frac{n-1}{n(n+1)}, \quad \delta\gamma_{gq}^{(0)n} = -4C_F \frac{n+2}{n(n+1)} \\
 \delta\gamma_{gg}^{(0)n} &= 4C_A \left[2S_1(n) - \frac{4}{n(n+1)} - \frac{11}{6} \right] + \frac{8}{3}T_f
 \end{aligned} \tag{A.1}$$

where $C_F = 4/3$, $C_A = 3$ and $T_f = f/2$, with f being the number of active flavors ($f = 3$ has been used when calculating $\delta\gamma_{ij}$). Note that $\delta\gamma_{NS}^{(0)n} = \delta\gamma_{qq}^{(0)n} = \gamma_{qq}^{(0)n}$ where the latter quantity refers to the spin-averaged (unpolarized) anomalous dimension. Furthermore, for the first $n = 1$ moment we have $\delta\gamma_{qq}^{(0)1} = \delta\gamma_{qg}^{(0)1} = 0$ as a consequence of helicity conservation at the quark-gluon vertex.

The spin-dependent NLO ($\overline{\text{MS}}$) two-loop flavor non-singlet anomalous dimensions $\delta\gamma_{NS}^{(1)n}(\eta)$, required in (2.10) for the evolution of $\delta q_{NS\eta=\pm}^n(Q^2)$, are the same as found for the spin-averaged case, $\delta\gamma_{NS}^{(1)n}(\eta) = \gamma_{NS}^{(1)n}(\eta)$ with $\gamma_{NS}^{(1)n}(\eta = \pm 1)$ being given by eq.(B.18) of [36]. Note that $\delta\gamma_{NS}^{(1)n}(\eta = +1)$ governs the evolution of the NS combinations $\delta q - \delta\bar{q}$, while $\delta\gamma_{NS}^{(1)n}(\eta = -1)$ refers to the combinations $\delta q + \delta\bar{q}$ appearing in the NS expressions (2.11). The NLO flavor singlet anomalous dimensions $\delta\gamma_{ij}^{(1)n}$ in the $\overline{\text{MS}}$ scheme are as follows [11]:

$$\delta\gamma_{qq}^{(1)n} = \gamma_{NS}^{(1)n}(\eta = -1) + \delta\gamma_{PS,qq}^{(1)n} \tag{A.2}$$

with $\gamma_{NS}^{(1)n}(\eta = -1)$ being again given by eq.(B.18) of [36] and⁵

$$\delta\gamma_{PS,qq}^{(1)n} = 16C_F T_f \frac{n^4 + 2n^3 + 2n^2 + 5n + 2}{n^3(n+1)^3} \quad (\text{A.3})$$

$$\begin{aligned} \delta\gamma_{qg}^{(1)n} &= 8C_F T_f \left[2 \frac{n-1}{n(n+1)} \left(S_2(n) - S_1^2(n) \right) + 4 \frac{n-1}{n^2(n+1)} S_1(n) \right. \\ &\quad \left. - \frac{5n^5 + 5n^4 - 10n^3 - n^2 + 3n - 2}{n^3(n+1)^3} \right] \\ &+ 16C_A T_f \left[\frac{n-1}{n(n+1)} \left(-S_2(n) + S_2' \left(\frac{n}{2} \right) + S_1^2(n) \right) - \frac{4}{n(n+1)^2} S_1(n) \right. \\ &\quad \left. - \frac{n^5 + n^4 - 4n^3 + 3n^2 - 7n - 2}{n^3(n+1)^3} \right] \end{aligned} \quad (\text{A.4})$$

$$\begin{aligned} \delta\gamma_{gq}^{(1)n} &= 32C_F T_f \left[-\frac{n+2}{3n(n+1)} S_1(n) + \frac{5n^2 + 12n + 4}{9n(n+1)^2} \right] \\ &+ 4C_F^2 \left[2 \frac{n+2}{n(n+1)} \left(S_2(n) + S_1^2(n) \right) - 2 \frac{3n^2 + 7n + 2}{n(n+1)^2} S_1(n) \right. \\ &\quad \left. + \frac{9n^5 + 30n^4 + 24n^3 - 7n^2 - 16n - 4}{n^3(n+1)^3} \right] \\ &+ 8C_A C_F \left[\frac{n+2}{n(n+1)} \left(-S_2(n) + S_2' \left(\frac{n}{2} \right) - S_1^2(n) \right) + \frac{11n^2 + 22n + 12}{3n^2(n+1)} S_1(n) \right. \\ &\quad \left. - \frac{76n^5 + 271n^4 + 254n^3 + 41n^2 + 72n + 36}{9n^3(n+1)^3} \right] \end{aligned} \quad (\text{A.5})$$

$$\begin{aligned} \delta\gamma_{gg}^{(1)n} &= 8C_F T_f \frac{n^6 + 3n^5 + 5n^4 + n^3 - 8n^2 + 2n + 4}{n^3(n+1)^3} \\ &+ 32C_A T_f \left[-\frac{5}{9} S_1(n) + \frac{3n^4 + 6n^3 + 16n^2 + 13n - 3}{9n^2(n+1)^2} \right] \\ &+ 4C_A^2 \left[-S_3' \left(\frac{n}{2} \right) - 4S_1(n)S_2' \left(\frac{n}{2} \right) + 8\tilde{S}(n) + \frac{8}{n(n+1)} S_2' \left(\frac{n}{2} \right) \right. \\ &\quad \left. + 2 \frac{67n^4 + 134n^3 + 67n^2 + 144n + 72}{9n^2(n+1)^2} S_1(n) \right. \\ &\quad \left. - \frac{48n^6 + 144n^5 + 469n^4 + 698n^3 + 7n^2 + 258n + 144}{9n^3(n+1)^3} \right] \end{aligned} \quad (\text{A.6})$$

where

$$S_k(n) \equiv \sum_{j=1}^n \frac{1}{j^k}$$

⁵ Note that $\delta P_{ij}^{(0,1)}(x) \rightarrow P_{ij}^{(0,1)}(x)$ as $x \rightarrow 1$ (or equivalently $\delta\gamma_{ij}^{(0,1)n} \rightarrow \gamma_{ij}^{(0,1)n}$ as $n \rightarrow \infty$) except for $\delta P_{gq}^{(1)}(x) > P_{gq}^{(1)}(x)$ as $x \rightarrow 1$. This latter property has, however, no quantitative consequences for the positivity, eq.(1.3), of our resulting NLO parton distributions.

$$\begin{aligned}
S'_k\left(\frac{n}{2}\right) &\equiv 2^{k-1} \sum_{j=1}^n \frac{1+(-)^j}{j^k} \\
&= \frac{1}{2}(1+\eta)S_k\left(\frac{n}{2}\right) + \frac{1}{2}(1-\eta)S_k\left(\frac{n-1}{2}\right) \\
\tilde{S}(n) &\equiv \sum_{j=1}^n \frac{(-)^j}{j^2} S_1(j) \\
&= -\frac{5}{8}\zeta(3) + \eta \left[\frac{S_1(n)}{n^2} + \frac{\zeta(2)}{2}G(n) + \int_0^1 dx x^{n-1} \frac{\text{Li}_2(x)}{1+x} \right] \quad (\text{A.7})
\end{aligned}$$

with $G(n) \equiv \psi\left(\frac{n+1}{2}\right) - \psi\left(\frac{n}{2}\right)$ and $\eta \equiv (-)^n \rightarrow \pm 1$ for $\delta\gamma_{NS}^{(1)n}(\eta = \pm 1)$ and $\eta \rightarrow -1$ for the flavor singlet anomalous dimensions (evolutions). The analytic continuations in n , required for the Mellin inversion of these sums to Björken- x space, are well known [16].

It should be noted that the original results for $\delta\gamma_{ij}^{(1)n}$ have been presented [11] in terms of multiple sums, denoted by $\tilde{S}_k(n)$, $S_{k,l}(n)$ and $\tilde{S}_{k,l}(n)$, which cannot be directly analytically continued in n . The following relations have been used in order to arrive at (A.4)-(A.6):

$$\begin{aligned}
\tilde{S}_k(n) &\equiv \sum_{j=1}^n \frac{(-)^j}{j^k} \\
&= \frac{1}{2^{k-1}} S'_k\left(\frac{n}{2}\right) - S_k(n) \\
S_{1,2}(n) + S_{2,1}(n) &\equiv \sum_{i=1}^n \left[\frac{1}{i} S_2(i) + \frac{1}{i^2} S_1(i) \right] \\
&= S_1(n)S_2(n) + S_3(n) \\
\tilde{S}_{1,2}(n) &\equiv \sum_{i=1}^n \frac{1}{i} \tilde{S}_2(i) \\
&= S_1(n)\tilde{S}_2(n) + \tilde{S}_3(n) - \tilde{S}(n) \quad (\text{A.8})
\end{aligned}$$

where for the latter sum we have used the identity

$$\sum_{i=1}^n \sum_{j=1}^i a_{ij} = \sum_{i=1}^n \sum_{j=1}^n a_{ij} - \sum_{j=1}^n \sum_{i=1}^{j-1} a_{ij}$$

in order to relate $\tilde{S}_{1,2}$ to the expressions in (A.7).

Finally, the first $n = 1$ moments of the $q \rightarrow q(\bar{q})$ and $g \rightarrow q(\bar{q})$ transitions reduce to [11, 37]

$$\delta\gamma_{NS}^{(1)1}(\eta = -1) = 0, \quad \delta\gamma_{qq}^{(1)1} = 24C_F T_f, \quad \delta\gamma_{qg}^{(1)1} = 0 \quad . \quad (\text{A.9})$$

References

- [1] M. Glück, E. Reya and W. Vogelsang, Phys. Lett. **B359**, 201 (1995).
- [2] H.J. Lipkin, Phys. Lett. **B256**, 284 (1991); **B337**, 157 (1994);
J. Lichtenstadt and H.J. Lipkin, Phys. Lett. **B353**, 119 (1995).
- [3] M.J. Alguard et al., SLAC-Yale Collab. (E80), Phys. Rev. Lett. **37**, 1261 (1976);
G. Baum et al., Phys. Rev. Lett. **45**, 2000 (1980);
G. Baum et al., SLAC-Yale Collab. (E130), Phys. Rev. Lett. **51**, 1135 (1983).
- [4] J. Ashman et al., EMC, Phys. Lett. **B206**, 364 (1988); Nucl. Phys. **B328**, 1 (1989).
- [5] D. Adams et al., SMC, Phys. Lett. **B329**, 399 (1994); Erratum **B339**, 332 (1994).
- [6] K. Abe et al., SLAC-E143 Collab., Phys. Rev. Lett. **74**, 346 (1995) and SLAC-PUB-6508 (1994); Phys. Lett. **B364**, 61 (1995). From the latter reference we have taken only those data points which correspond to the new beam energies of 9.7 and 16.2 GeV and to $Q^2 > 0.6 \text{ GeV}^2$.
- [7] B. Adeva et al., SMC, Phys. Lett. **B302**, 533 (1993);
D. Adams et al., SMC, Phys. Lett. **B357**, 248 (1995).
- [8] D.L. Anthony et al., SLAC-E142 Collab., Phys. Rev. Lett. **71**, 959 (1993);
F. Staley, SLAC-E142 Collab., Proc. of the Int. Europhysics Conf. on High Energy Physics, Marseille, France, 1993, eds. J. Carr and M. Parrottet, p.114.
- [9] K. Abe et al., SLAC-E143 Collab., Phys. Rev. Lett. **75**, 25 (1995) and SLAC-PUB-95-6734.
- [10] M. Gourdin, Nucl. Phys. **B38**, 418 (1972);
J. Ellis and R.L. Jaffe, Phys. Rev. **D9**, 1444 (1974); Erratum **D10**, 1669 (1974).
- [11] R. Mertig and W.L. van Neerven, Univ. Leiden INLO-PUB-6/95 and NIKHEF-H/95-031, June 1995, November 1995 (revised version);
W. Vogelsang, RAL-TR-95-071, November 1995 (Phys. Rev. D), where the revised Mertig - van Neerven results were confirmed.

- [12] For some recent discussions see, e.g., M. Anselmino, A. Efremov, and E. Leader, CERN-TH. 7216/94 (Phys. Rep., to appear).
- [13] W. Furmanski and R. Petronzio, Z. Phys. **C11**, 293 (1982).
- [14] M. Glück, E. Reya, and A. Vogt, Z. Phys. **C67**, 433 (1995).
- [15] M. Glück, E. Reya, and W. Vogelsang, Nucl. Phys. **B351**, 579 (1991).
- [16] M. Glück, E. Reya, and A. Vogt, Z. Phys. **C48**, 471 (1990).
- [17] M. Glück, E. Reya, and A. Vogt, Phys. Rev. **D45**, 3986 (1992).
- [18] G. Altarelli, Proc. of the 27th Int. E. Majorana Summer School of Subnuclear Physics, Erice 1989, Plenum Press 1990 [CERN-TH.5675/90]; Proc. of the HERA-Workshop, Hamburg 1991, eds. W. Buchmüller and G. Ingelman, DESY, 1992, vol. I, p.379.
- [19] E. Reya, Schladming lectures 1993, Springer Lecture Notes in Physics **426**, 175 (1994).
- [20] L. Mankiewicz and A. Schäfer, Phys. Lett. **B242**, 455 (1990);
L. Mankiewicz, Phys. Rev. **D43**, 64 (1991);
W. Vogelsang, Z. Phys. **C50**, 275 (1991).
- [21] G. Altarelli and G.G. Ross, Phys. Lett. **B212**, 391 (1988);
A.V. Efremov and O.V. Teryaev, Dubna report E2-88-287, 1988 [published in the Proceedings of the Int. Hadron Symposium, Bechyne, Czechoslovakia, 1988, eds. J. Fischer et al. (Czech. Academy of Science, Prague, 1989), p.302].
- [22] R.D. Carlitz, J.C. Collins, and A.H. Mueller, Phys. Lett. **B214**, 229 (1988).
- [23] G. Altarelli and B. Lampe, Z. Phys. **C47**, 315 (1990).
- [24] M. Glück and E. Reya, Phys. Rev. **D25** 1211 (1982).
- [25] Particle Data Group, L. Montanet et al., Phys. Rev. **D50**, 1173 (1994);
F.E. Close and R.G. Roberts, Phys. Lett. **B316**, 165 (1993).
- [26] J. Ellis and M. Karliner, Phys. Lett. **B313**, 131 (1993).

- [27] G. Altarelli, P. Nason, and G. Ridolfi, Phys. Lett. **B320**, 152 (1994); Erratum **B325**, 538 (1994).
- [28] T. Gehrmann and W.J. Stirling, Z. Phys. **C65**, 461 (1995).
- [29] R.D. Ball, S. Forte, and G. Ridolfi, Nucl. Phys. **B444**, 287 (1995).
- [30] M. Glück, E. Reya, and A. Vogt, Z. Phys. **C53**, 127 (1992); Phys. Lett. **B306**, 391 (1993).
- [31] S.J. Brodsky and I. Schmidt, Phys. Lett. **B234**, 144 (1990);
S.J. Brodsky, M. Burkhardt, and I. Schmidt, Nucl. Phys. **B441**, 197 (1995);
F.E. Close and D. Sivers, Phys. Rev. Lett. **39**, 1116 (1977).
- [32] M. Glück, E. Reya, and W. Vogelsang, Nucl. Phys. **B239**, 347 (1990).
- [33] M. Glück, R.M. Godbole, and E. Reya, Z. Phys. **C41**, 667 (1989).
- [34] M.A. Ahmed and G.G. Ross, Nucl. Phys. **B111**, 441 (1976).
- [35] G. Altarelli and G. Parisi, Nucl. Phys. **B126**, 298 (1977).
- [36] E.G. Floratos, C. Kounnas and R. Lacaze, Nucl. Phys. **B192**, 417 (1981).
- [37] J. Kodaira, Nucl. Phys. **B165**, 129 (1979).

Figure Captions

Fig.1 Comparison of our NLO and LO results for $A_1^N(x, Q^2)$ as obtained from the fitted inputs at $Q^2 = \mu_{NLO,LO}^2$ for the 'standard' (eqs.(3.7) and (3.7')) scenario with present data [4-9]. The Q^2 values adopted here correspond to the different values quoted in [4-9] for each data point starting at $Q^2 \gtrsim 1 \text{ GeV}^2$ at the lowest available x -bin. The results in the 'valence' scenario are indistinguishable from the ones shown.

Fig.2 The Q^2 -dependence of $A_1^{p,d}(x, Q^2)$, as predicted by the NLO and LO QCD evolutions at various fixed values of x , compared with recent SLAC-E143 [6] (solid circles) and SMC data [5, 7] (open circles).

Fig.3 The Q^2 -dependence of $A_1^{p,n}(x, Q^2)$ as predicted by the NLO and LO QCD evolutions at various fixed values of x .

Fig.4a Comparison of our 'standard' and 'valence' NLO and LO results with the data [4-9] for $g_1^d(x, Q^2)$. The SMC data correspond to different $Q^2 \gtrsim 1 \text{ GeV}^2$ for $x \geq 0.005$, as do the theoretical results.

Fig.4b Same as in Fig.4a but for $g_1^n(x, Q^2)$. The E142 and E143 data [8, 9] correspond to an average $\langle Q^2 \rangle = 2$ and 3 GeV^2 , respectively, and the theoretical predictions correspond to a fixed $Q^2 = 3 \text{ GeV}^2$.

Fig.5a Comparison of our fitted 'standard' and 'valence' input NLO ($\overline{\text{MS}}$) densities in eqs.(3.7) and (3.8) with the unpolarized dynamical input densities of ref.[14].

Fig.5b The same as in Fig.5a but for the LO input densities according to eqs.(3.7') and (3.8').

Fig.6 The polarized LO and NLO ($\overline{\text{MS}}$) densities at $Q^2 = 4 \text{ GeV}^2$, as obtained from the input densities at $Q^2 = \mu_{NLO,LO}^2$ in Figs.5a,b. In the 'standard' scenario, δs coincides with the curves shown for $\delta \bar{q}$ in NLO and LO due to the $SU(3)_f$ symmetric input which is only marginally broken in NLO for $Q^2 > \mu_{NLO}^2$.

Fig.7 The experimentally allowed range of NLO polarized gluon densities at $Q^2 = 4 \text{ GeV}^2$ for the 'valence' scenario with differently chosen $\delta g(x, \mu_{NLO}^2)$ inputs. The 'fitted δg '

curve is identical to the one in Fig.6 and corresponds to $\delta g(x, \mu_{NLO}^2)$ in eq.(3.8). Very similar results are obtained if $\delta g(x, \mu_{NLO}^2)$ is varied accordingly within the 'standard' scenario as well as in a LO analysis (see, e.g., ref.[1]).

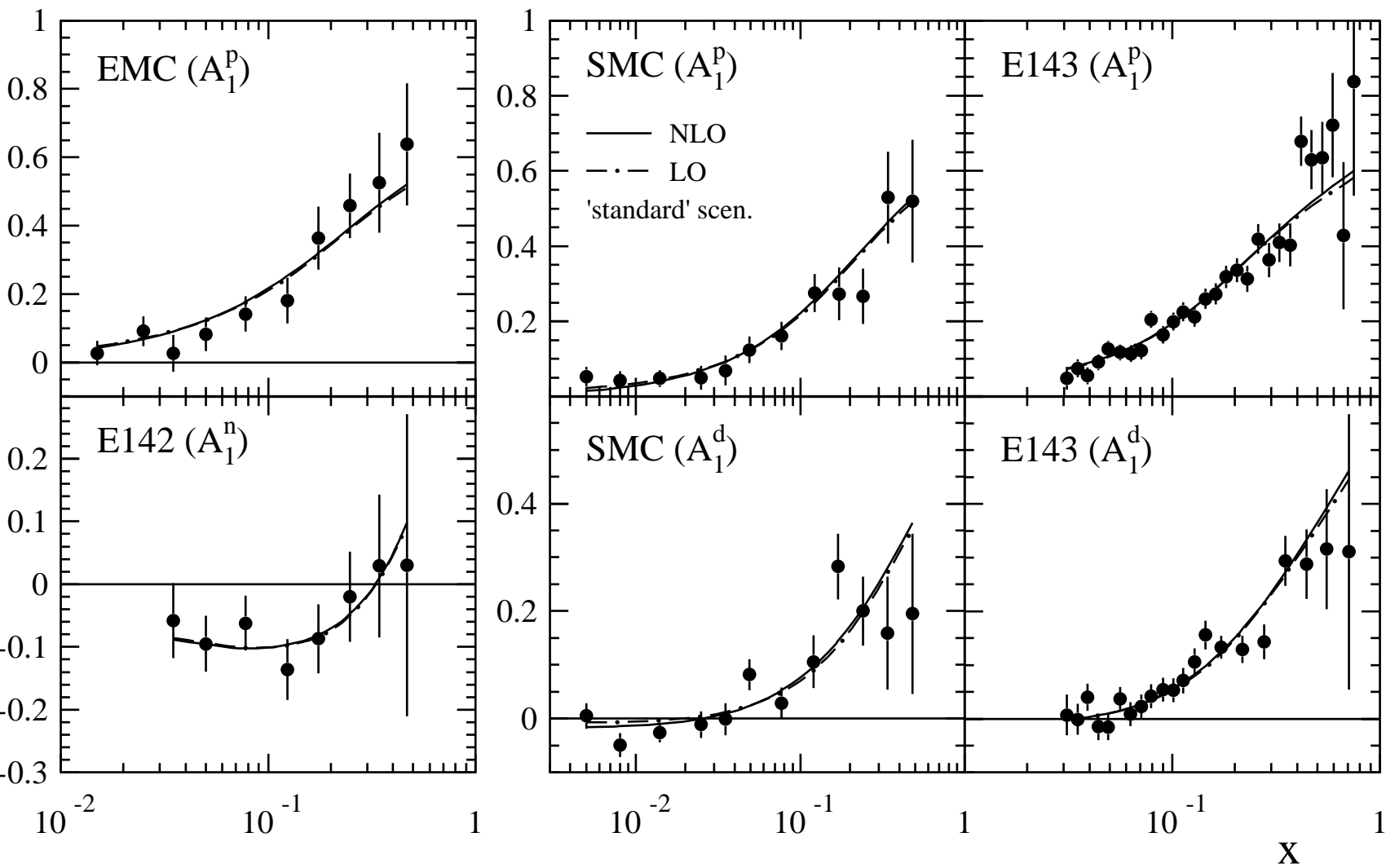


Fig. 1

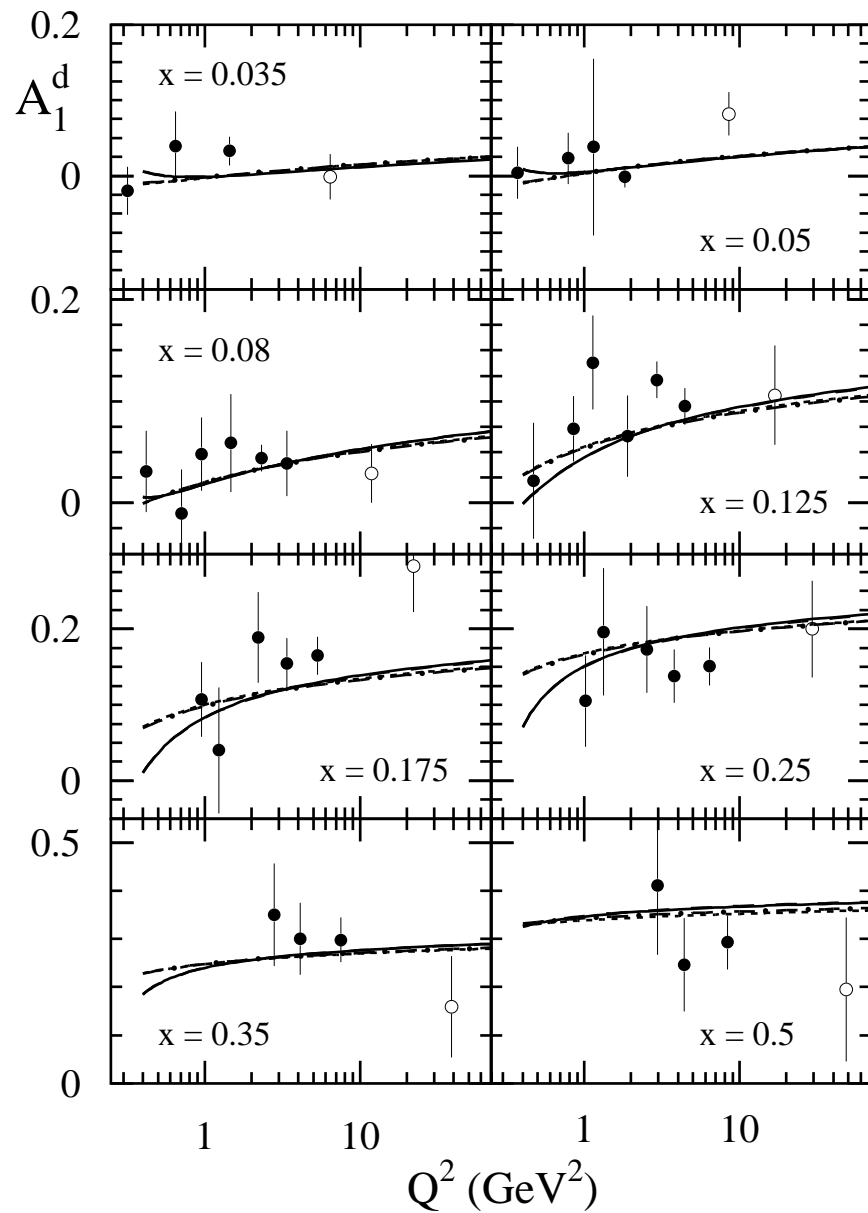
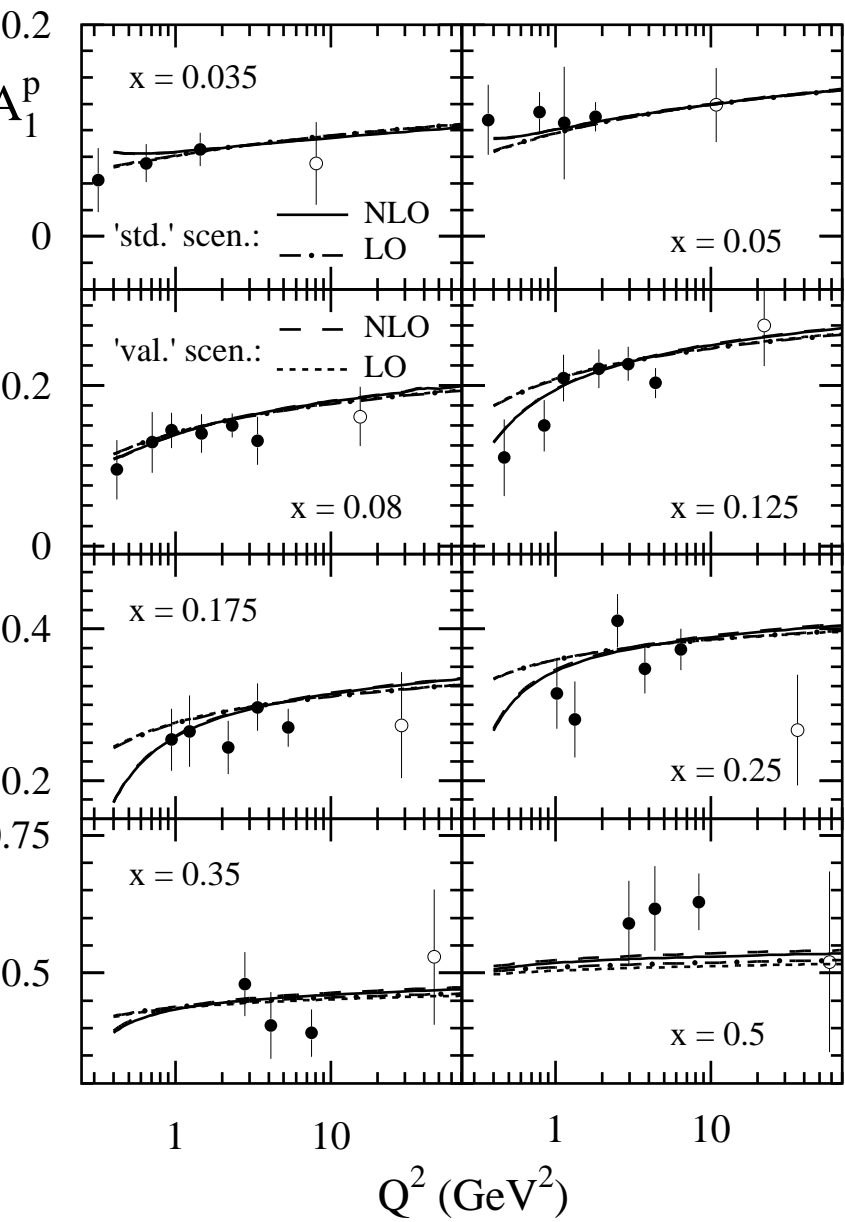


Fig. 2

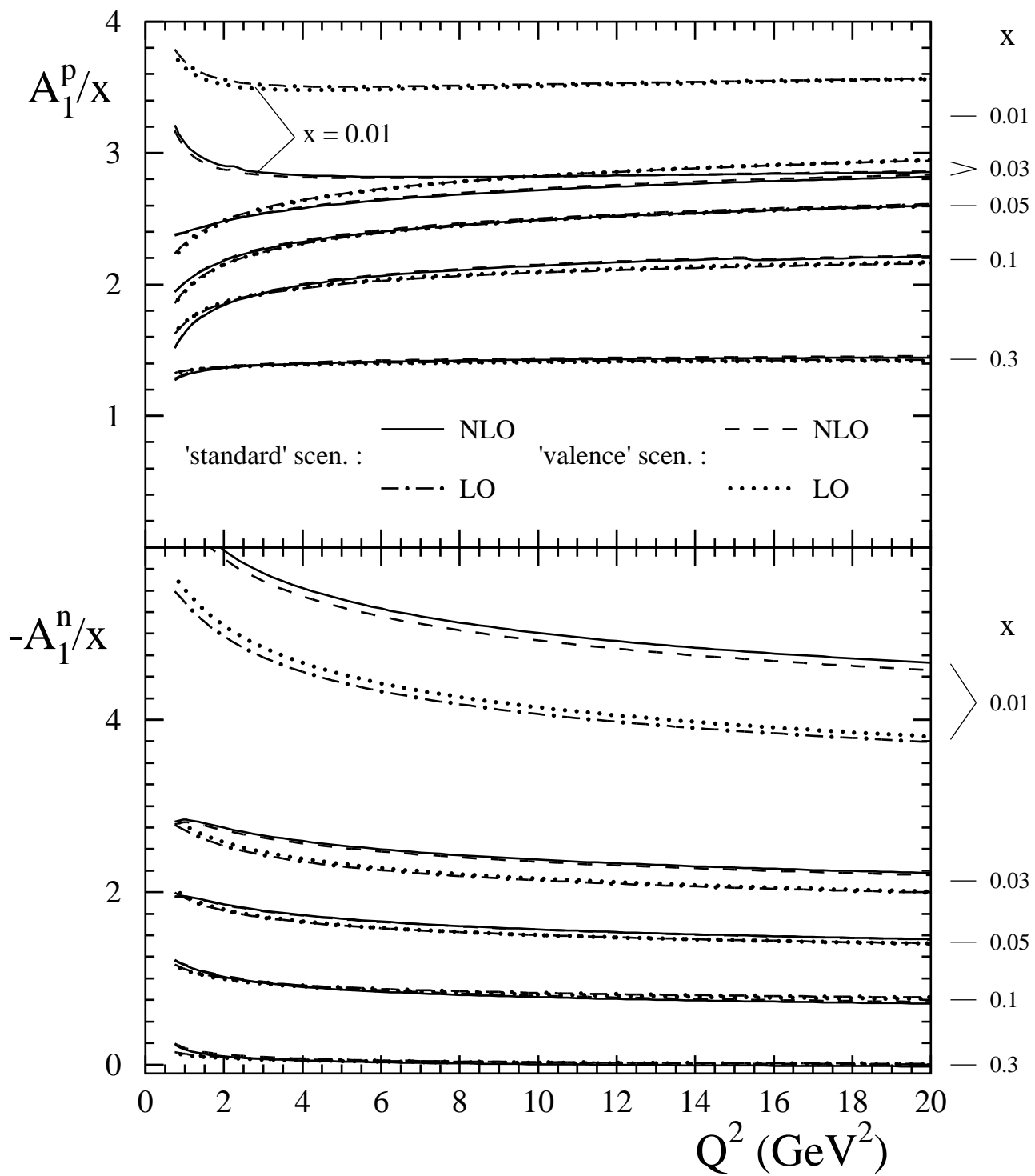


Fig. 3

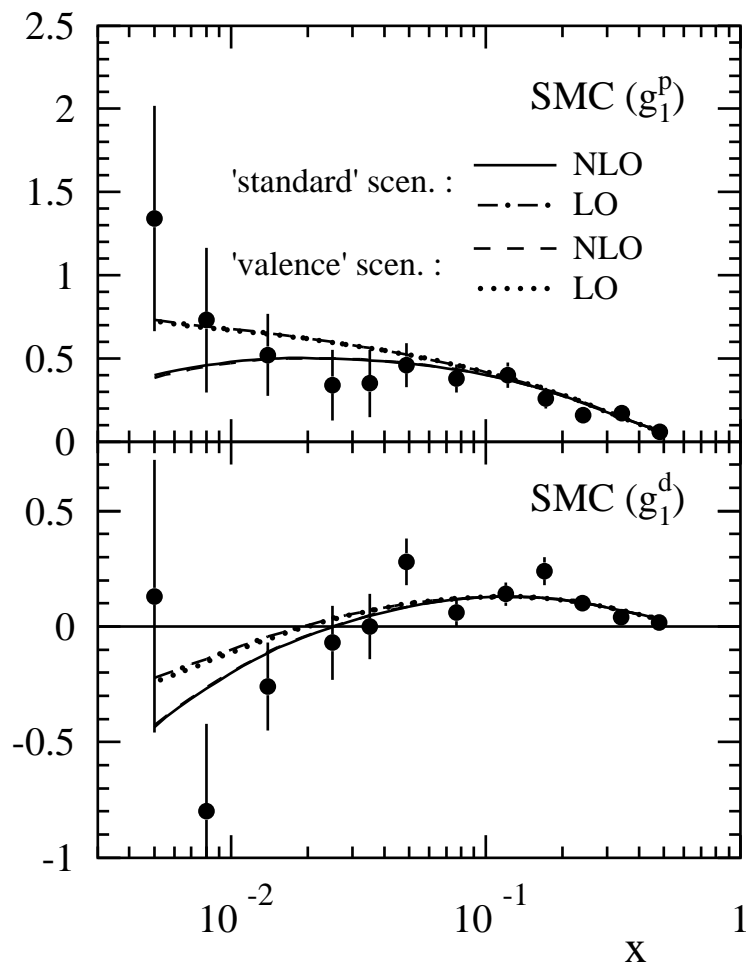
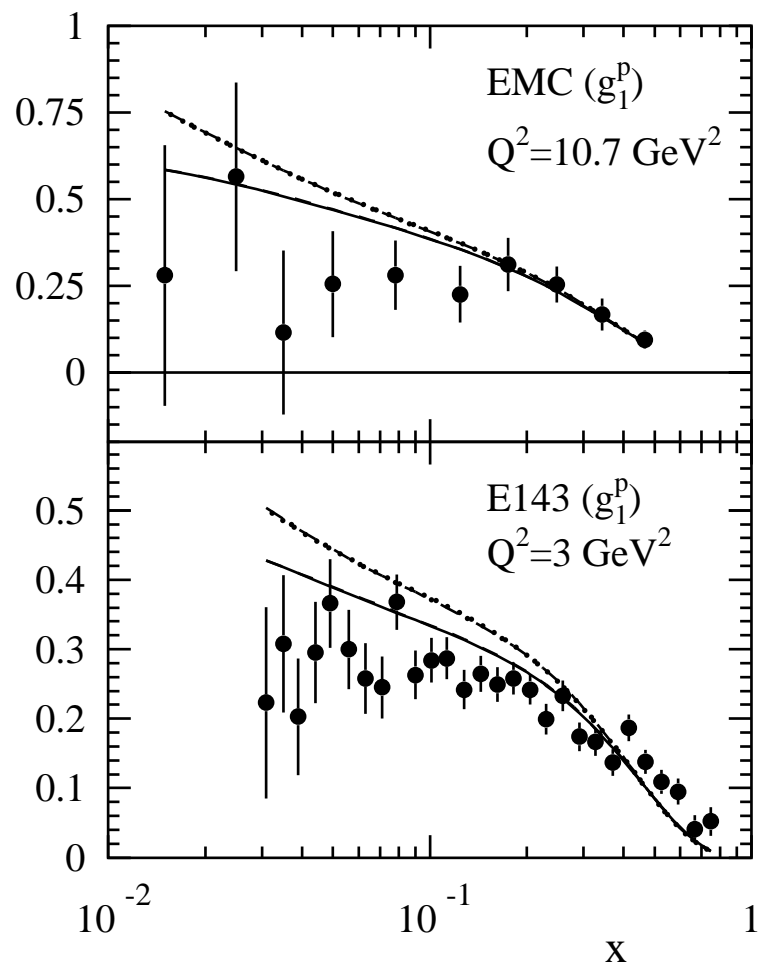


Fig. 4a

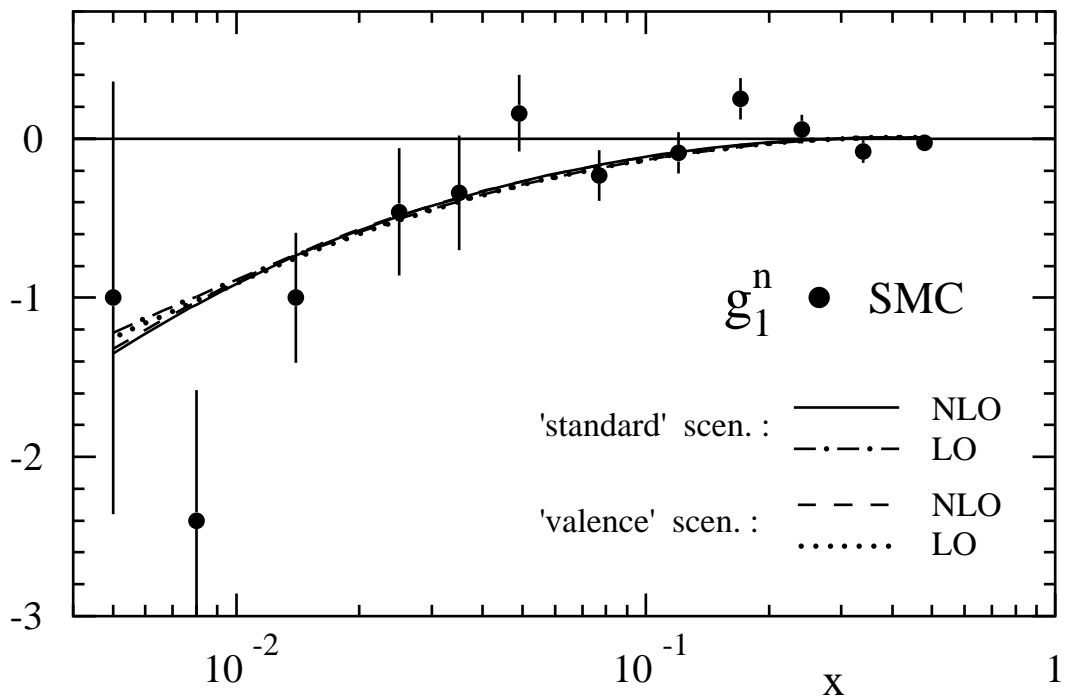
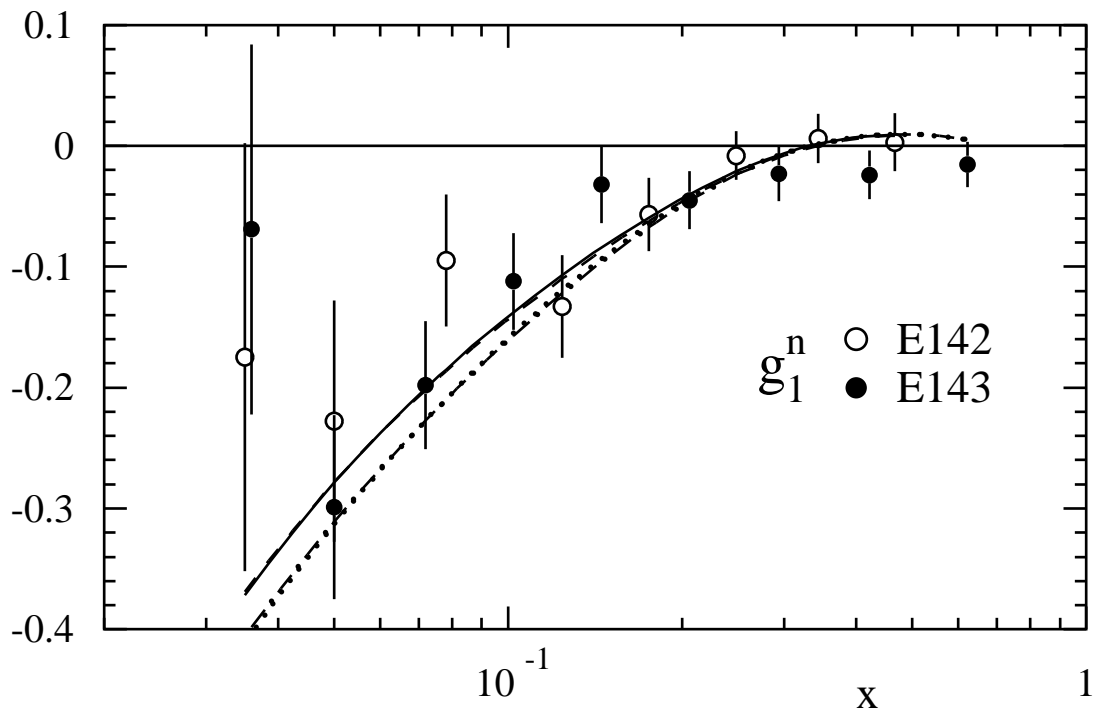


Fig. 4b

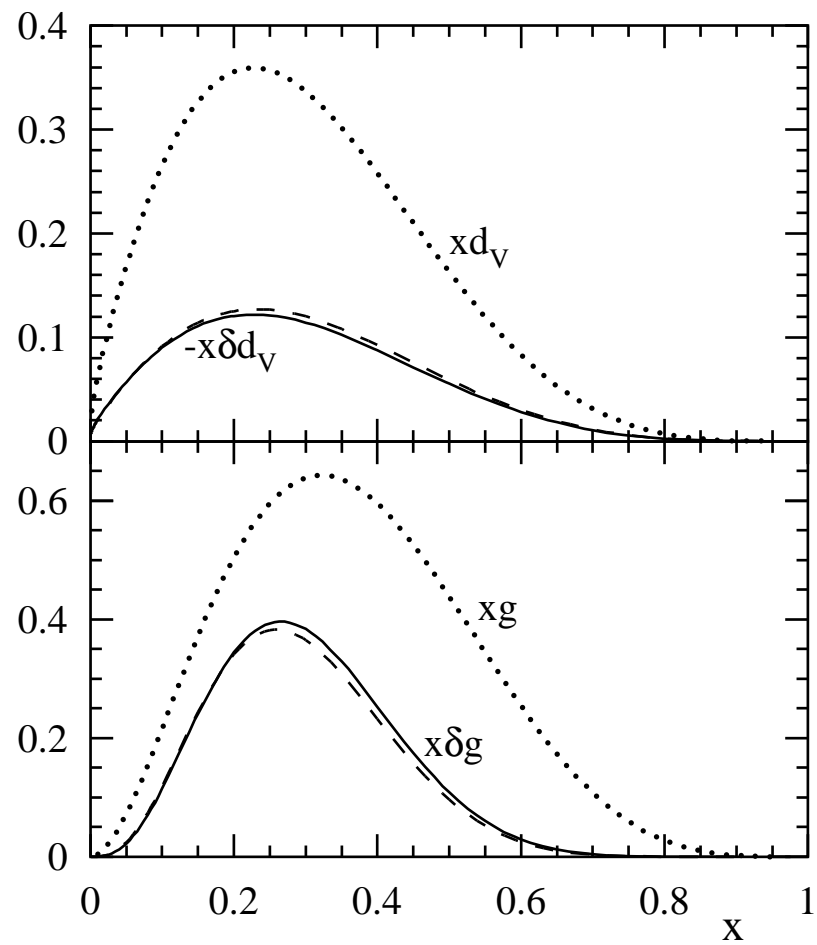
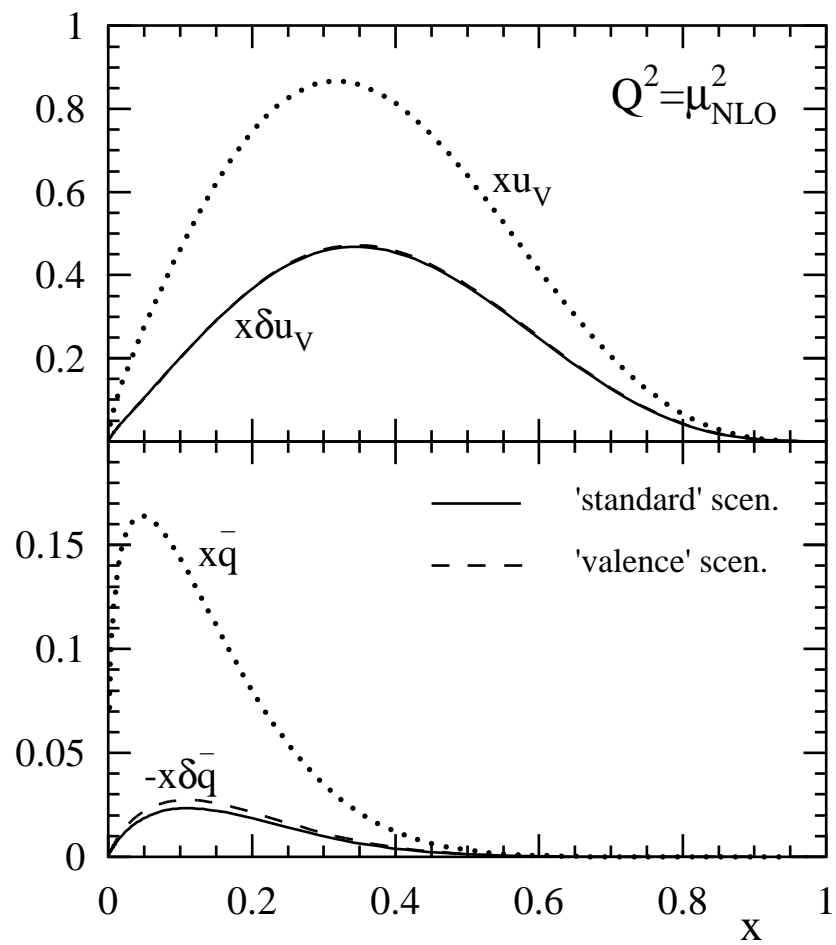


Fig. 5a

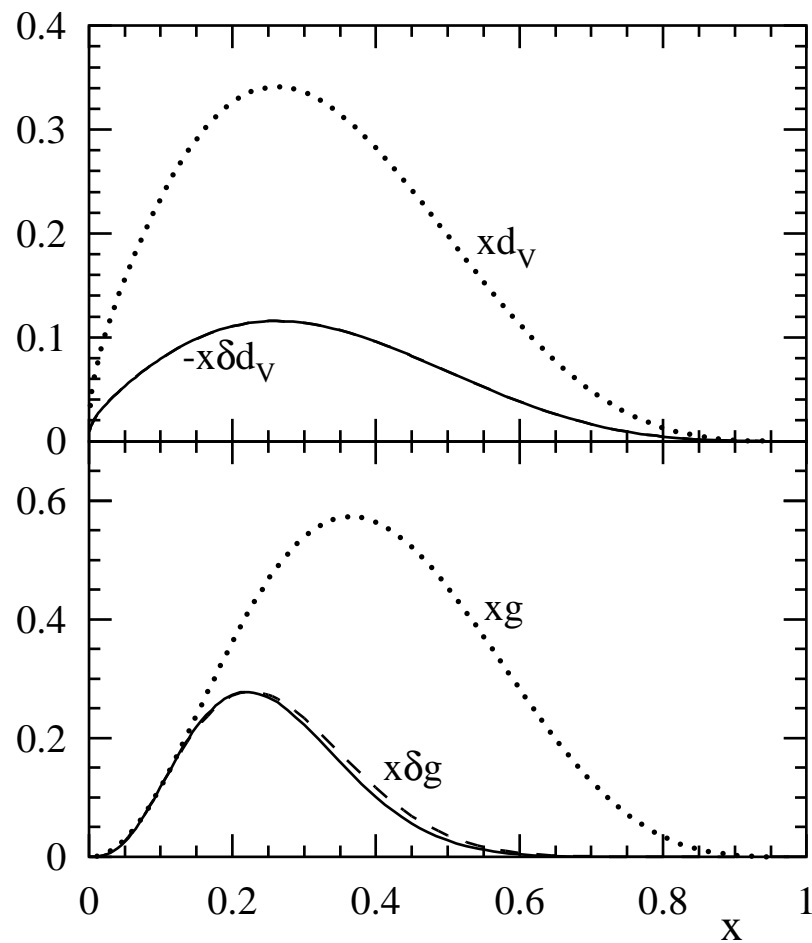
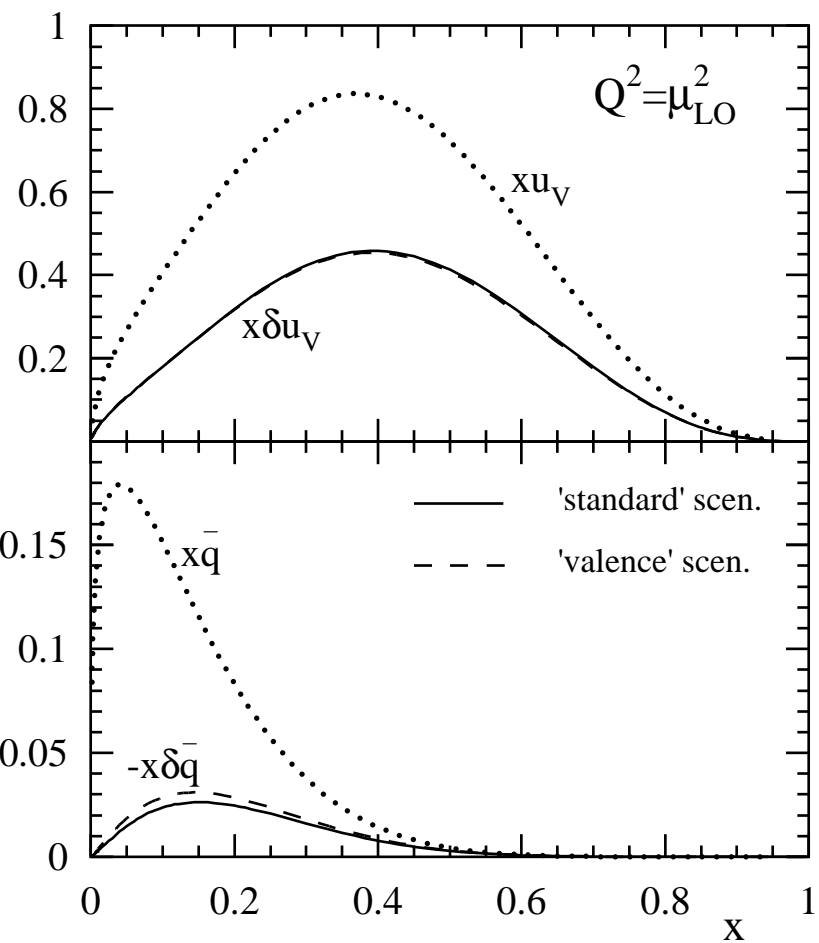


Fig. 5b

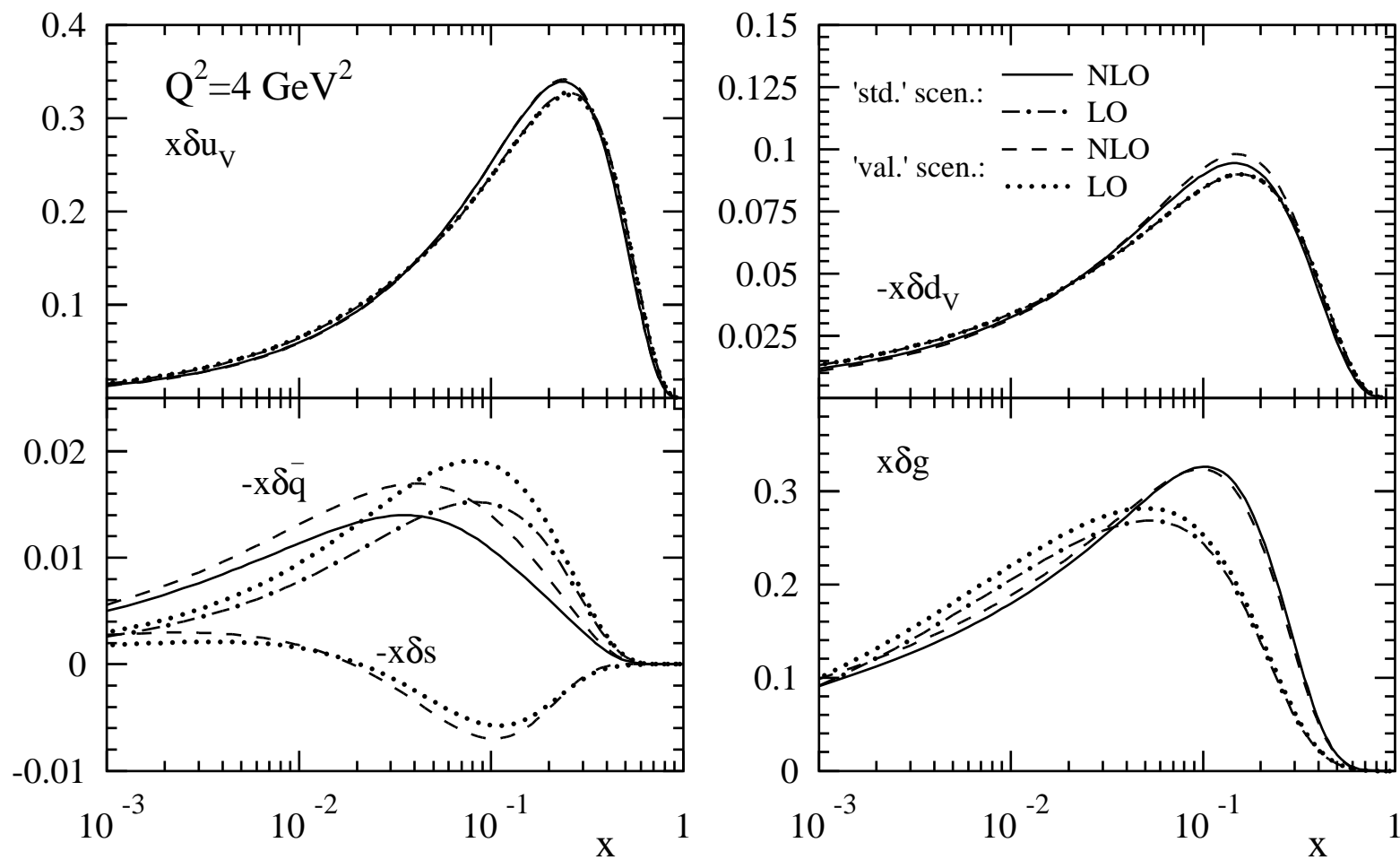


Fig. 6

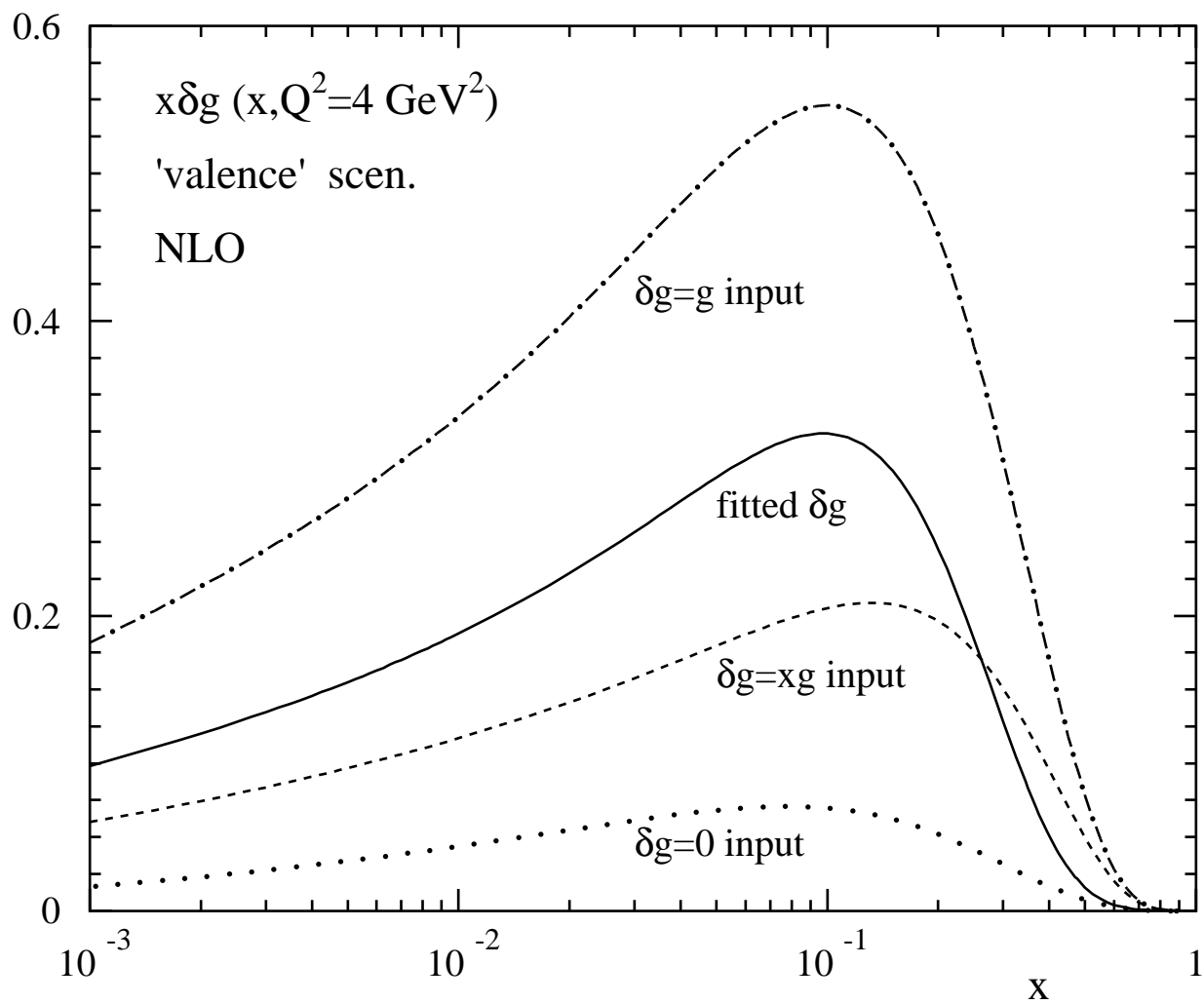


Fig. 7